THESIS FOR THE DEGREE OF DOCTOR OF PHILOSOPHY

On the Formation and Physical Behaviour of Exhaled Particles

HELENE HOLMGREN

Department of Chemical and Biological Engineering
CHALMERS UNIVERSITY OF TECHNOLOGY
Göteborg, Sweden 2011

On the Formation and Physical Behaviour of Exhaled Particles
HELENE HOLMGREN
ISBN 978-91-7385-593-8

Doktorsavhandlingar vid Chalmers tekniska högskola
Ny serie nr 3274
ISSN 0346-718X

Department of Chemical and Biological Engineering
Chalmers University of Technology
SE-412 96 Göteborg, Sweden
Telephone: +46 (0)31 772 1000

This document is written in LaTeX

Printed by Chalmers Reproservice
Göteborg, Sweden 2011

On the Formation and Physical Behaviour of Exhaled Particles
HELENE HOLMGREN
Department of Chemical and Biological Engineering
Chalmers University of Technology

Abstract

Aerosol particles are generated in human airways and leave the body with exhaled air. The particles originate from the respiratory tract and contain non-volatile compounds that potentially may be used as biomarkers for various medical conditions. To utilise any information provided by the particles, they must be characterised. The work performed in this thesis focuses on measuring concentrations and size distributions of endogenous particles in exhaled air. The results give indications on how and where in the airways particles are formed.

Number size distributions of exhaled particles, obtained from different individuals and breathing techniques, were measured. The results show that the inter-individual variation in number concentration is very high, while the size distribution peaks at about the same diameter for all subjects. The distribution peaks at a smaller particle diameter for tidal breathing than it does for breathing reaching airway closure. Moreover, deep exhalations result in significantly higher particle concentrations than tidal breathing. Exhalation followed by a few seconds breath hold amplifies the number of particles emitted in the subsequent exhalation, whereas breath hold after inhalation reduces the concentration. It was also found that a particle quickly shrinks when it leaves the saturated environment inside the human body for a surrounding with lower relative humidity.

The results obtained support the theory that exhaled particles are created through a film rupture process. Following exhalation, airway closure and subsequent inhalation, fluid films are spanned across the airways. These films burst and form particles that leave the body with the next exhalation. It is suggested that tidal breathing activates the very smallest airways and produces the smallest particles. As exhalation depth increases, additional, larger airways close and larger particles are formed. Breath hold at low lung volume results in extensive airway closure and increased particle concentration, while breath hold at high lung volume causes deposition and loss of particles. It is further suggested that the particles are supersaturated liquid droplets shortly after leaving the human body.

Keywords: exhaled particles, size distribution, tidal breathing, airway closure, relative humidity, breath hold, deposition, film droplet

List of Papers

This thesis is based on the work presented in the following papers, which are referred to in the text by their Roman numerals (I-IV).

I. **H. Holmgren**, E. Ljungström, A.-C. Almstrand, B. Bake and A.-C. Olin. Size Distribution of Exhaled Particles in the Range from 0.01 to 2.0 μm. *Journal of Aerosol Science.* 2010:41:439-446.

II. **H. Holmgren**, B. Bake, A.-C. Olin and E. Ljungström. Relation between Humidity and Size of Exhaled Particles. *Journal of Aerosol Medicine and Pulmonary Drug Delivery.* 2011:24:253-260.

III. **H. Holmgren**, E. Gerth, E. Ljungström, A.-C. Almstrand, P. Larsson, B. Bake and A.-C. Olin. Effects of Breath Holding at Low and High Lung Volumes on Amount of Exhaled Particles. Manuscript.

IV. **H. Holmgren** and E. Ljungström. Influence of Film Dimensions on Film Droplet Formation. Accepted for publication in *Journal of Aerosol Medicine and Pulmonary Drug Delivery*.

In **Paper I**, **Paper II** and **Paper IV**, I designed and performed the experiments, with support from my supervisor. I am main responsible for data evaluation and interpretation. In **Paper III**, I took part in designing the experiments on breath hold at high lung volume. I collected, evaluated and interpreted all data concerning that part of the study.

Contents

List of Abbreviations

Abbreviation	Description	Definition
CP	closing point	page 8
CPC	condensation particle counter	page 27
CV	closing volume	page 8
DMA	differential mobility analyser	page 26
ERV	expiratory reserve volume	page 7
EBC	exhaled breath condensate	page 1
FEV_1	forced expiratory flow in one second	page 8
FRC	functional residual capacity	page 7
IRV	inspiratory reserve volume	page 7
OPC	optical particle counter	page 25
RTLF	respiratory tract lining fluid	page 5
RV	residual volume	page 7
SDFC	specific droplet formation capacity	page 23
SEM	scanning electron microscope	page 30
SMPS	scanning mobility particle sizer	page 28
TLC	total lung capacity	page 8
TV	tidal volume	page 7
VC	vital capacity	page 7

Introduction

It has been known for a considerable time that aerosol particles are generated in human airways, and that these particles leave the body as we cough, sneeze, laugh, speak, or even as we breathe. The particles contain non-volatile compounds, presumably originating from the respiratory tract lining fluid (RTLF) in one or several regions of the airways.[1−4] Exhaled particles may carry pathogens that transmit airborne infectious diseases.[5,6] In addition, their potential as carriers of indicators of various diseases and lung conditions is discussed in the literature.[1,3,4,7]

Recent interest in endogenously produced exhaled particles was partly sparked by the observation of non-volatile, biogenic compounds in exhaled breath condensate (EBC).[3,4,7,8] EBC is obtained by cooling exhaled air and collecting the condensed water in a receiver. The only way that non-volatile material can end up in the receiver is if it is transported from the exhaling subject in the form of airborne particles. In addition to water, EBC contains every type of molecule that RTLF does, but in very low concentrations. Many potential biomarkers for airway inflammation and oxidative stress, originating from RTLF, have been detected in EBC.[3,4,7,8] Unfortunately, EBC equipment is not often designed for efficient particle collection. Consequently, this way of collecting non-volatile material from exhaled breath has been troubled with, e.g., contamination, unpredictable dilution of the samples, and concentrations close to the detection limit.[3,4,7−9] A more efficient methodology is required to utilise any information provided by the non-volatile compounds in exhaled breath. Such a method should focus on collecting particles, and for this purpose it is crucial to understand the formation mechanisms and physical behaviour of these particles.

The work described in this thesis was undertaken with the overall aim to extend the knowledge about the physical behaviour of exhaled aerosol particles. The intention was to better understand where in the airways formation takes place, and which mechanisms govern the formation. This thesis is based on four scientific papers. Number size distributions of exhaled particles in the range from 0.01 to 2.0 μm, obtained from different individuals and different breathing techniques, are measured in **Paper I**. This is, to the author's knowledge, the first time size distributions of exhaled particles smaller than 0.4 μm have been measured with good size resolution.

In **Paper II**, the relation between humidity and size of exhaled particles is experimentally investigated. By measuring number size distributions of exhaled particles at various relative humidities, it is possible to estimate the corresponding size distribution at the point of generation, i.e., at high relative humidity. **Paper III** examines how it is possible to influence the concentrations of particles being emitted from an individual by altering the breathing pattern. The results are important not only for the basic understanding of particle formation, but they can also help improve the process of collecting exhaled particles for chemical analysis. In **Paper IV**, fluid films are spanned across holes of different diameters. These films burst, in analogy with soap bubbles, and droplets are formed. The influence of film dimensions on droplet formation is investigated, with possible implications for exhaled particle formation.

To put the results presented in the papers in context, a **Background** to the field of interest is presented. This includes an overview of the respiratory system and a brief introduction to the fundamental physical properties of aerosol particles. The phenomenon of exhaled particles is introduced. The appended papers are based on experimental studies presented in the **Material and Methods** section. Also described are the commercial instruments that were used in the studies. A summary of the **Results** obtained in each paper is presented, and subsequently debated in the **Discussion**. Finally, I give some **Concluding Remarks and Outlook** for future work.

Background

The Respiratory System

The Airways

The main function of the lungs is to enable gas exchange, i.e., to transport oxygen to the bloodstream and carbon dioxide from the bloodstream. The respiratory system, illustrated in Figure 1, can be divided into three main regions: the conducting zone, the transitional zone and the respiratory zone. The conducting zone comprises airways that conduct gas to and from the respiratory zone, where the exchange of oxygen and carbon dioxide takes place. Between the conducting zone and the respiratory zone is the transitional zone, in which both air flow and gas exchange occur.

The conducting zone consists of trachea, bronchi and bronchioles. The trachea divides into left and right primary bronchus. The primary bronchi subsequently branch off to form smaller secondary bronchi, which in turn divide into even smaller bronchi. Trachea and primary bronchi are supported by semi-circular cartilage, but as the diameter of the bronchi decreases, the cartilage rings are replaced by irregularly shaped cartilage plates. The plates diminish progressively in the distal airways and disappear when the airways are approximately 1 mm in diameter. By definition, airways without cartilage are termed bronchioles.[10,11] Glands exist in the conducting airways, and all inner walls are lined with ciliated epithelium that catch debris and remove it in the mucus escalator. The smallest bronchiole that is still completely lined by bronchial epithelial cells is the terminal bronchiole.[12]

In the transitional zone, alveoli begin to appear in the airway wall. Alveoli are small, thin-walled and compliant air sacs with a rich capillary blood supply. They are designed specifically for gas exchange. Alveoli are attached to all parts of the region, and ciliated cells extend from the main bronchi to the bronchioloalveolar junction. These cilia are short and decreased in number, but their function is maintained.[12]

The respiratory zone begins where the walls of the airways are entirely made of alveoli, and the bronchiolar epithelial cells have completely disappeared. The alve-

olar duct terminates in alveolar sacs, which are clusters of alveoli. Gas exchange occurs via diffusion, moving gas from the alveolar sacs across the alveolar and capillary walls into the capillary blood. There are between 300 and 800 million alveoli in the lungs, covering a surface area of 70-90 m^2.[11,13,14] Even though the respiratory zone is not ciliated, inhaled particles that are deposited there may be cleared out by resident macrophages.

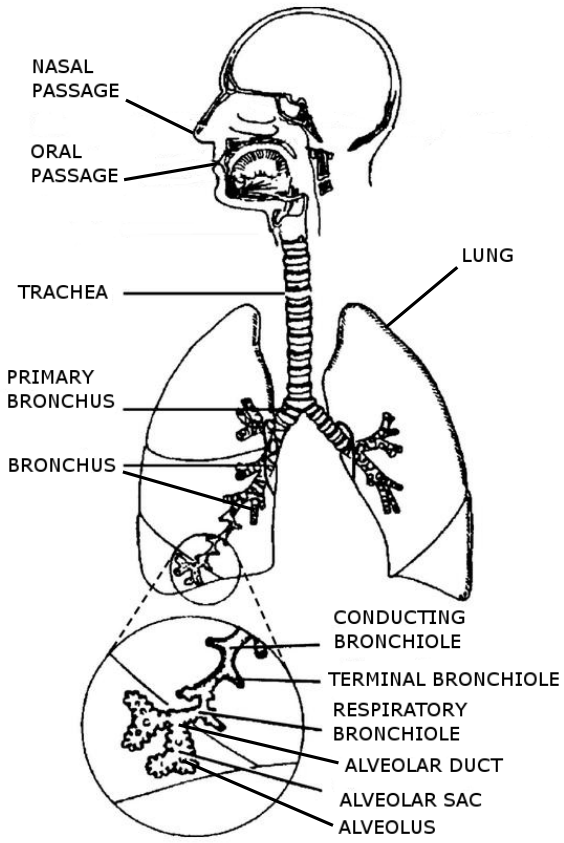

Figure 1: The respiratory system. Adapted from Hinds.[14]

Each level of branching in the airways is called a generation. At each bifurcation, the cross-sectional area of a daughter branch is decreased by a factor of about 0.75.[12] The trachea is generation $z = 0$, and the primary bronchi are generation $z = 1$. The first sixteen generations, from trachea to terminal bronchioles, make up the conducting zone. The transitional zone includes the next three generations, where the number of alveoli in the airway wall steadily increases. Finally, there are three generations of alveolar ducts and one generation of alveolar sacs, which constitute the respiratory zone. Airways of generation 8 and above are often called small airways or peripheral airways. Table 1 gives the characteristics of the respiratory system, as formulated by Weibel[15] and adapted by Hinds.[14] Even though Weibel describes the respiratory system as symmetrical, the branching pattern is actually significantly asymmetrical.[16]

Table 1: Characterisation of the respiratory system. The table is based on Weibel's generally accepted lung model and constructed from information by Weibel[15] and Hinds.[14]

airway	generation z	number per generation n(z)	diameter cm	length cm	total cross section cm^2
trachea	0	1	1.8	12.0	2.54
primary bronchus	1	2	1.22	4.76	2.33
lobar bronchus	2	4	0.830	1.90	2.13
	3	8	0.560	0.76	2.00
segmental bronchus	4	16	0.450	1.27	2.48
	5	32	0.350	1.07	3.11
	6	64	0.280	0.90	3.96
	7	128	0.230	0.76	5.10
bronchi with cartilage in wall	8	256	0.186	0.64	6.95
	9	512	0.154	0.54	9.56
	10	1024	0.130	0.46	13.4
terminal bronchus	11	2048	0.109	0.39	19.6
	12	4096	0.095	0.33	28.8
	13	8192	0.082	0.27	44.5
bronchioles with muscles in wall	14	16384	0.074	0.23	69.4
	15	32768	0.066	0.20	113.0
terminal bronchiole	16	65536	0.060	0.165	180.0
respiratory bronchiole	17	131072	0.054	0.141	300.0
	18	262144	0.050	0.117	534.0
	19	524288	0.047	0.099	944.0
alveolar duct	20	1048576	0.045	0.083	1600.0
	21	2097152	0.043	0.070	3220.0
	22	4194304	0.041	0.059	5880.0
alveolar sac	23	8388608	0.041	0.050	11800.0

Respiratory Tract Lining Fluid (RTLF)

Respiratory tract lining fluid (RTLF) is a thin liquid film that lines the air-facing surface of the lungs. It lubricates and protects the pulmonary epithelium and is critical for maintaining the normal lung functions and lung structure. For example, the surface tension that acts on the air RLTF interface is responsible for 50-60% of the lung's elastic recoil.[17] Moreover, RTLF can react with inhaled gas and thereby influence gas transfer.[18] RTLF is distributed continuously throughout the respiratory tract, but its chemical composition, cellular constituents and physiology varies between the conducting zone and the respiratory zone.[19]

The conducting zone is lined with a $\sim$5-100 μm thick layer of RTLF.[19] In this region, the fluid is believed to consist of two phases:[20] a periciliary watery sol which surrounds the epithelial cilia, and a covering mucus blanket or gel. The gel phase contains bronchial glycoproteins, some serum proteins and protein bound to the

bronchial glycoproteins, while the sol phase contains any soluble components of bronchial secretion, together with serum proteins.[21] RTLF constitutes a mechanical barrier to inhaled particles and microorganisms. Generally, particles with diameters larger than about 5 μm are trapped in the lining fluid and are then cleared from the lung via the mucociliary escalator. Here, the cilia beat the mucus towards the mouth, thus propelling inhaled particles and mucus up to the oropharynx for swallowing or expectoration.

RTLF in the respiratory zone is a watery phase covered by an overlying film of surfactant, about 0.1-0.2 μm deep.[19] The pulmonary surfactant is composed of phospholipids ($\sim$80%), cholesterol ($\sim$10%), proteins ($\sim$10%) and small amounts of carbohydrates.[19] The lipid composition is dominated by phosphatidylcholine, but there are also significant amounts of phosphatidylglycerol present. Inhaled particles that are smaller than about 5 μm in diameter and pass through the conducting zone can be trapped in the alveolar RTLF. Here, they become available for phagocytosis by resident alveolar macrophages. The macrophages physically remove the phagocytised material from the alveoli to the mucosciliary escalator of the conducting zone or across the alveolar epithelium to the interstitium or circulating blood.

Lung and airway diseases, such as asthma, cystic fibrosis, acute respiratory distress syndrome and pneumonia, are associated with alterations of the RTLF composition.[22–25] By identifying and quantifying the compounds in RTLF, it may therefore be possible to detect and diagnose lung and airway diseases, as well as to monitor patients and follow up on pharmaceutical treatments.

The Ventilation Cycle

A normal, healthy adult processes between 10 and 20 m^3 air per day.[14] Normal respirations are 10 to 18 breaths per minute, with about 0.5 litres of air being inhaled and exhaled with each breath. During forceful breathing, e.g. during heavy work, respirations can be 40 breaths per minute, and the volume of air in a breath may reach 6 litres. The breathing cycle is driven by active muscle labour as well as by passive forces.[11,26] Inhalation is an active process, initiated by the diaphragm and supported by external intercostal muscles. The lung volume increases when the diaphragm contracts and the rib cage expands. Contents of the abdomen are moved downward. During exhalation, the muscles relax and the lung volume decreases by passive forces. If breathing is forced, expiratory muscles assist in the recoil. The internal intercostal muscles and the abdominal muscles cause the ribcage to depress and the thorax, lungs and alveoli to contract. Under normal conditions, however, alveoli contract due to recoil of the surrounding elastic fibres. Lung recoil is also an effect of surface fluid forces in the lung.[11,26] The pulmonary surfactant found in RTLF reduces the surface tension in the alveoli, thus lowering the elastic recoil and increasing lung compliance. The normal surface tension of water is about 72 mN m^{-1},[27] and in the

lungs it is 25 mN m^{-1}.[11,26] However, at the end of expiration, compressed surfactant phospholipid molecules reduce the surface tension to near-zero levels. The presence of surfactant thus prevents a collapse of the alveoli during expiration by reducing the surface tension. Furthermore, the reduction in surface tension draws fluid across the alveolar wall, reducing fluid accumulation in the alveoli.

Surfactant also helps regulate alveolar size.[11,26] During inhalation, alveoli increase in size and the surfactant is spread out over a larger surface. As a consequence, surface tension increases, and the expansion rate of the alveoli decreases. This means that all alveoli will expand at the same rate, since a large alveolus will experience a large increase in surface tension and its expansion will be slowed down. Likewise, the rate of alveolar shrinking becomes more regular during exhalation, due to the presence of surfactant.

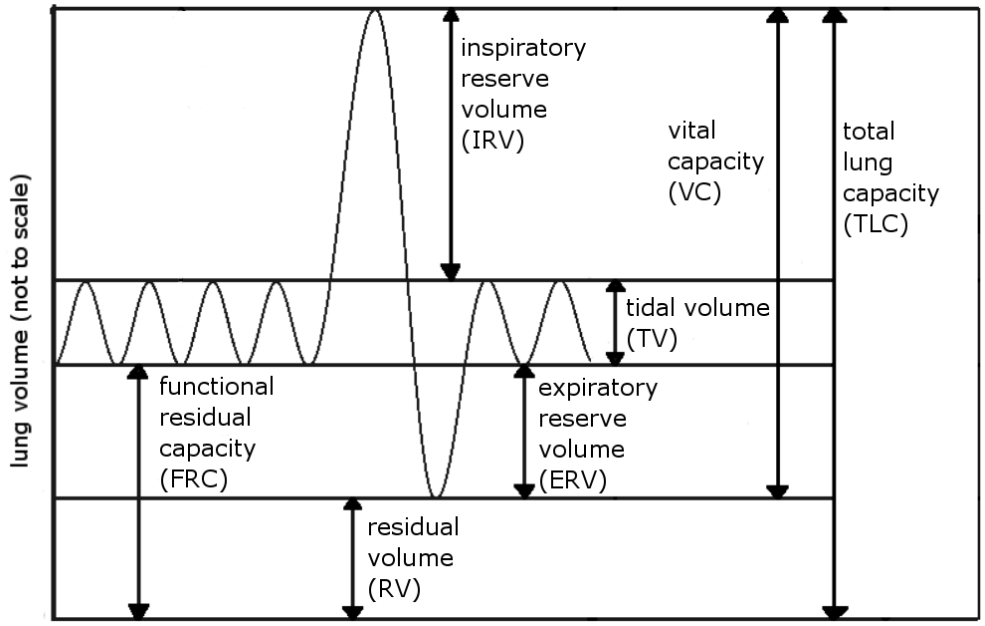

Figure 2: Lung volumes and capacities.

Lung volume refers to the volume of air associated with different phases of the ventilation cycle. Lung volumes and capacities are illustrated in Figure 2. Tidal volume (TV) is the volume of air that is inhaled or exhaled during a breath, at rest. This type of breathing is referred to as tidal breathing. Inspiratory reserve volume (IRV) is the additional volume that can be inhaled, by force, following a normal inspiration. Conversely, expiratory reserve volume (ERV) is the additional volume that can be exhaled, by force, following a normal expiration. Vital capacity (VC) is the maximum volume of air that can be exhaled after a maximal inspiration; VC = TV + IRV + ERV. Residual volume (RV) is the volume of air still in the lungs at the end of a maximal expiration; RV = FRC - ERV. It cannot be expired no matter how vigorous the effort. Functional residual capacity (FRC) is the volume of air remaining in the

lungs at the end of a normal expiration; FRC = RV + ERV, and total lung capacity (TLC) is the volume of air in the lungs at the end of a maximal inspiration; TLC = FRC + TV + IRV + RV.

Lung volumes are important for assessing lung function. The most commonly used units are FRC, VC and FEV_1, which can be measured using spirometry. FEV_1 - forced expiratory flow in one second - is the volume of air that can be expired during one second after a maximum inspiration. A low FEV_1/FVC value indicates airway obstruction.

Airway Closure

Airway closure is a phenomenon that involves blockage of the airways. It takes place at low lung volume in healthy adults, normally at the end of an expiration approaching RV.[28,29] The liquid blockages usually rupture during the subsequent inspiration, and the re-opening of airways can be identified by a crackling sound, detectable by sensitive instruments.[30,31] It is suggested that airway closure occurs in the vicinity of the terminal bronchioles, where airway diameters are small and the RTLF layer is thick.[28,29] The fundamental features of airway closure were first described by Dollfuss et al.[32] in 1967. The authors showed that closure of peripheral airways begins in the lower lung regions (while in upright position), and progresses toward the upper lung regions with further decrease in lung volume. The point at which airway closure begins during a progressive slow exhalation is called the closing point (CP), and the volume remaining to residual volume is the closing volume (CV). Tidal airway closure can be observed in, e.g., chronic obstructive pulmonary disease, asthma, obesity and chronic heart failure.[33] Further, elderly subjects generally reach airway closure earlier than younger individuals.[32,34] This observation has been attributed to age-related loss of lung recoil,[34] but it has also been suggested that a decreased resistance to collapse of aged airways plays a role.[33]

Kamm and Schroter[35] distinguish between two types of airway closure, which they define as compliant collapse and film collapse. In compliant collapse, the airway walls are deformed by compression and held in apposition by the adhesive properties of RTLF.[17,35,36] This type of collapse is promoted by flexibility of the airway walls and high surface tension of the RTLF layer.[17,35–37] Film collapse is described as liquid plug formation in rigid axisymmetric vessels. It is a purely fluid-mechanical process which tends to occur when the surface tension is much smaller than the airway wall stiffness,[17] and the ratio of lining fluid thickness to airway radius is high.[35–36] At the end of a deep expiration, surface tension driven instabilities in the RTLF lead to the formation of liquid plugs that occlude the airways.[17,29,32,35] During this process, the airway walls remain more or less cylindrical. In excised dog lungs, compliant collapse is the most likely process,[38] but it still appears unknown which type of collapse that dominates in human lungs.

The tendency to form plugs in the airways is still being investigated, and the mechanism is not yet fully understood. Cassidy et al.[39] combined studies of immiscible liquids flowing in a capillary with theoretical considerations and concluded that a high surface tension of the liquid and a high ratio of liquid layer thickness to capillary diameter promote instability and plug formation in axisymmetric capillaries. Malashenko et al.[40] hypothesised that the liquid plug that forms inside small airways will travel along the airway, and disintegrate if the capillary number is high. The capillary number is a dimensionless number expressing the ratio of hydrodynamic shear forces to surface tension at a gas liquid interface.[40] Lindsley et al.[41] and Heil et al.[17] considered the likely possibility that airways and lining before and after closure are not axisymmetric but adapt more realistic geometries.

Aerosol Particles

Aerosols are defined as suspensions of liquid or solid particles in a gas. The term particle or particulate matter is used for either solid or liquid particles in the aerosol. When the particle is liquid, the term droplet is also used. Aerosols can be both natural and anthropogenic in origin. Some examples of particles originating from natural aerosol sources are sea spray, soil dust, fog, haze and mist. Anthropogenic aerosol sources are many, amongst others fossil fuel combustion and biomass burning. Worth mentioning are also bioaerosols, which are aerosols of biological origin, e.g., viruses, bacteria, spores, pollen and fungi.

Aerosol Characterisation

The behaviour of aerosols is largely characterised by particle size, which ranges from about 0.001 to over 100 μm in diameter. The lower end represents a freshly nucleated cluster, which contains only a few molecules, while the upper end would be the size of very fine sand. Particles are often referred to as having a diameter, even though they are not always spherical. The diameter of an aerosol particle is therefore a physical, rather than geometrical, property. An equivalent diameter is defined as the diameter of a sphere that would have the same value of a particular physical property as an irregularly-shaped object. Various types of instruments report different measures of particle diameter, depending on the employed methodology and application. Hence, a universal measure of particle size does not exist.

Aerosol particles are normally measured by number or mass concentration. Number concentrations of particles emphasize the numerous, but tiny particles, while mass concentrations are biased towards larger and heavier particles. Sometimes, measurements focus on surface area or volume. The type of measurement chosen is based on the effect of the particle that is in focus. For spherical particles of known density, it is easy to convert between mass, number, volume and surface concentrations.

Most aerosols are polydisperse, i.e., contain particles of different sizes. It is therefore necessary to introduce size distributions, e.g., number size distributions or mass size distributions. To obtain a number size distribution, the entire size range of the aerosol is divided into a series of successive size intervals, and the number of particles in each interval is determined. The size groups must be contiguous, with the upper size limit of each interval coinciding with the lower size limit of the next interval. To be able to compare contents of intervals with different widths, the number of particles in an interval is often divided by the width of the size interval in which they are found. This gives the number of particles per unit of size interval, e.g., number μm^{-1}. By using a large number of intervals, a smooth size distribution is obtained. This smooth curve may be amendable to mathematical interpretation. For example, the area under the number size distribution curve is proportional to the number concentration of particles. A size distribution can also be described with the y-axis giving the fraction of particles in each interval. This is the frequency function of the aerosol. The area under the frequency function between particle diameter d_i and d_{i+1} equals the fraction of particles whose diameters fall within this interval.

Aerosols may sometimes be described by the normal (or Gaussian) distribution. All normal distributions are symmetrical and have a bell-shaped density curve with a single peak located at a mean value. The probability function, *P(x)*, of a normal distribution can be described by Equation 1.

$$P(x) = \frac{1}{SD\sqrt{2\pi}} e^{-(x-\mu)^2/2SD^2} \tag{1}$$

Here, μ is the mean value of the distribution, where the peak of density occurs, and SD is the standard deviation, which gives the spread of the curve. For normally distributed particles, 95% of all particles fall within the size range defined by μ $\pm$2SD. Polydisperse aerosols with a large size span cannot be described by the normal distribution. Instead, the log-normal distribution is used, which is a normal distribution with the x-axis on logarithmic scale. The parameters in Equation 1 are then replaced with their logarithmic counterparts.

Aerosol Dynamics

When a particle is released in air, it quickly reaches its terminal settling velocity, V_{TS}. Here, the drag force by the air on the moving particle equals the opposite force of gravity. The terminal settling velocity for a spherical particle in still air and at Reynolds number (Re) < 0.1 can be described using Stokes's law in Equation 2,

$$V_{TS} = \frac{\rho_p d_p^2 g C_c}{18\eta}, \tag{2}$$

where η is absolute air viscosity, g is standard gravity, ρ_p is particle density, d_p is particle diameter, and C_c is the corresponding Cunningham slip correction factor. The

Cunningham slip correction factor is used to account for non-continuum effects when calculating the drag on small particles, and should be applied for particles < 1 μm.

Relaxation time, τ, is the time it takes for a particle released in still air to reach its terminal settling velocity. When the only external force acting on the particle is gravity, τ is defined as the ratio of terminal settling velocity to the acceleration of gravity. It can also be described as the product of particle mass, m, and mobility, B;

$$\tau = \frac{V_{TS}}{g} = mB. \tag{3}$$

The stopping distance, S, is the maximum distance a particle with initial velocity V_0 will travel in still air if no external forces are present, and can be described as

$$S = V_0\tau = mBV_0. \tag{4}$$

The value of S represents the ultimate distance a particle will travel in still air if any external forces acting on the particle were suddenly turned off. An important application for the stopping distance is for a particle moving with an airstream that is abruptly turned 90 degrees. In this case, the stopping distance is the distance the particle continues to travel in its original direction. Thus, it can be seen as a measure of the persistence of a particle to continue along its original path.[14]

The most important physical processes that affect aerosol dynamics are condensation, evaporation, deposition and coagulation.[14] Concepts that are central for the work performed in this thesis are described below.

Condensation and Evaporation

Aerosols are two-phase systems that include both particles and the gas in which the particles are suspended. The most important mass transfer processes between the gas phase and the particle phase are condensation and evaporation. Condensation can be described as a transition from gas to liquid phase that occurs when a vapour condenses on a pre-existing surface. Evaporation is the opposite process; a transition from liquid to vapour phase. During condensation, a particle grows bigger as it accumulates more liquid. When liquid evaporates from a particle, it will shrink. Condensation and evaporation only affect the properties of single particles, such as mass or size. As long as the particle is not completely removed by evaporation or transferred into a size that is not included in the measurement, the number concentration of particles will not change.

Particle growth by condensation normally requires a supersaturated vapour. Supersaturation may be produced by cooling a vapour, and is dependent on actual partial pressure, P, and saturation vapour pressure, P_S. P is the pressure that a gas (or vapour) in a mixture of gases would exert if it alone were to occupy the entire

volume that is now occupied by the mixture. P_S is a property of a bulk material, liquid or solid, that describes the pressure required to maintain a vapour in equilibrium with the condensed vapour at a specified temperature. When the partial pressure of a vapour equals its saturation vapour pressure, the system is in equilibrium. This means that the rate of evaporation from the surface equals the rate of condensation on the surface. If, at a given temperature, the partial pressure is less than the saturation vapour pressure, the vapour is unsaturated. If the partial pressure is greater than the saturation vapour pressure, it is supersaturated. The saturation ratio, S_R, is defined as the ratio between P and P_S, i.e., $S_R = P/P_S$. This means that for $S_R < 1$, the vapour is unsaturated, and for $S_R > 1$, it is supersaturated. For $S_R = 1$, the vapour is saturated.

The reasoning above applies to pure liquids. Aerosols are not often pure liquids, but contain a variety of chemical compounds. Raoult's law may then be applied to calculate the partial pressure P_i for the component i in a mixture.

$$P_i = P_i^0 \gamma x_i \tag{5}$$

Here, P_i^0 is the vapour pressure of the pure component i, x_i is the mole fraction of component i in the mixture, and γ is the activity coefficient, taking into account the non-ideality of the solution. Raoult's law states that the vapour pressure of a gas over a solution depends on the pure component vapour pressure and its mole fraction in the solution. As the total number of components in a solution increases, the individual vapour pressure decreases. Thus, a vapour may distribute into a particle made up of several components even though the vapour is not supersaturated.

If the liquid surface under consideration is curved, which is the case for droplets, the partial pressure required to maintain equilibrium is greater than that for a flat surface. Consequently, it is easier for molecules to evaporate from a droplet surface than from a flat surface. This is known as the Kelvin effect, and is significant for particles smaller than 0.1 μm in diameter.[14] The saturation ratio required for equilibrium in a pure liquid droplet is given by the Kelvin equation,

$$S_R = \frac{P}{P_S} = \exp\left(\frac{4\sigma M}{\rho R T d_k}\right), \tag{6}$$

where σ, M and ρ are surface tension, molecular weight and density of the liquid, and d_k is the droplet diameter that will neither grow nor evaporate at the given saturation ratio, i.e., the Kelvin diameter. T is the temperature of the system, and R is the gas constant. For every droplet diameter, there is a saturation ratio where the droplet is in equilibrium. If the ratio is too small, the droplet evaporates. If the ratio is too great, the droplet grows. An implication of the Kelvin effect is that small particles of pure liquid are unstable at saturation ($S_R = 1$) and will evaporate. A supersaturated environment is required to maintain equilibrium.

Deposition

Deposition of aerosol particles occurs mainly via sedimentation, diffusion, impaction, or interception.[14] These processes are illustrated in Figure 3. Other deposition mechanisms are electrostatic attraction, thermophoresis, diffusiophoresis and photophoresis, but these will not be discussed here.

Sedimentation, i.e., gravitational settling, means that a particle simply falls due to gravity. Sedimentation is the dominating deposition mechanism for particles larger than about 0.5 μm in diameter.[14] Diffusion is a primary transport mechanism for particles smaller than 0.1 μm and is seldom considered for particles larger than 1 μm.[14] It is the result of random movement of particles as they collide with gas molecules, i.e., Brownian motion. Gas molecules that undergo Brownian motion normally rebound when they hit a surface, but aerosol particles adhere to it and are lost. Impaction occurs when an obstacle is introduced into a flow of particles. The obstacle disturbs the gas flow and forces it to change direction. Small particles are able to follow the new direction of the flow, whereas large particles, owing to their greater inertia, are unable to change their direction and impact on the obstacle. Interception takes place when small particles, that originally follow the streamlines of an air flow, comes within one particle radius of the surface of an obstacle that is introduced in the flow. The edge of the particle collides with the obstacle and impacts because of its finite size. For a given particle size, there are certain streamlines that will result in interception, and other streamlines that will not. For pure interception, it is assumed that the particles have negligible inertia or Brownian motion, and that they follow the streamlines perfectly.

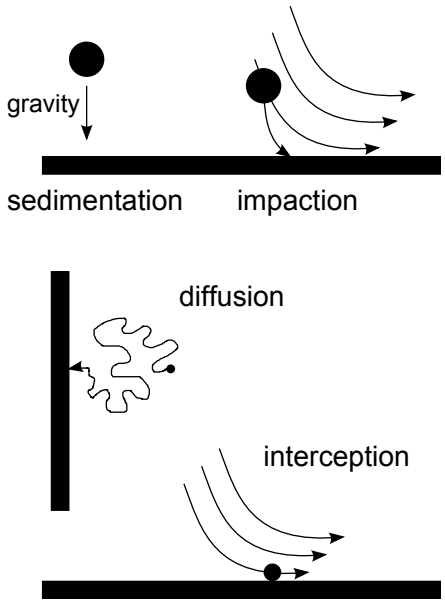

Figure 3: Particle deposition mechanisms.

Coagulation

Coagulation occurs when particles collide with each other and stick, forming new and larger particles in the process. Consequently, the total number of particles is reduced, while mass is conserved. Particles of the same size have a lower coagulation rate than particles of different sizes, since smaller particles often diffuse into the surface of larger ones. Thermal coagulation describes the process where the relative motion between particles is due to Brownian motion. In their random movement, particles may undergo numerous collisions with each other, depending on the number concentration of particles. This process is spontaneous and ever-present for aerosols. Kinematic coagulation is driven by other external forces than Brownian diffusion, such as gravity. Here, particles of different sizes settle at different rates, thereby creating relative motion between them. This leads to collision and coagulation.

Exhaled Particles

A minor natural source of aerosol particles, which is not yet fully understood, is exhaled breath from human beings. While the bulk matrix of exhaled air is a mixture of nitrogen, oxygen, carbon dioxide, water, and inert gases, a single breath also includes thousands of volatile and non-volatile compounds. The non-volatile compounds exit the body in the form of particles when we exhale.

Exhaled breath has been analysed for centuries, but the measurements have mainly focused on the volatile compounds. The ancient Greek physicians knew that they could diagnose diseases from the characteristic odour of a patient's breath. In the 17^{th} century, lung volume measurements were established as a diagnostic tool, mainly for tuberculosis. Nitric oxide (NO) is today a validated biomarker for airway inflammation, and current research investigates the use of volatile organic compounds (VOC) as biomarkers for lung cancer[42] and breast cancer.[43] Most inflammatory markers are, however, not volatile, and are therefore not found in the gas phase of exhaled aerosol.[9]

Low concentrations of non-volatile and semi-volatile substances, such as proteins and lipids, have been found in exhaled breath condensate (EBC). Many of the non-volatile compounds that have been found can be linked to airway inflammation and oxidative stress. Briefly, EBC is obtained by cooling moist exhaled air and collecting the condensate. Sampling EBC is easy, inexpensive and non-invasive. However, as mentioned in the introduction, the method has several disadvantages, such as unpredictable dilution of the samples and concentrations close to the detection limit.[3,7–9] Moreover, according to Bondesson et al.[44], EBC derives mainly from the central airways. This suggests that the method may not be appropriate for analysis of RTLF originating from smaller airways. A more efficient method is necessary to be able to utilise any information provided by the non-volatile compounds of exhaled air.

Such a method should focus on collecting exhaled particles, and for this purpose it is essential to understand the formation mechanism and physical behaviour of these particles.

Physical Analysis of Exhaled Particles

Early studies of endogenously produced particles in exhaled air indicated that the particles were in the super-micron range, but this can most likely be attributed to the fact that smaller particles could not be detected with the instruments that were used. One example is Jennison,[45] who in 1942 used high speed photography to measure droplets that were produced from sneezing and coughing. The smallest detectable diameter was 10 μm. Another early example is Duguid (1945),[46] who studied droplets produced from sneezing, coughing and speaking by microscopic measurements of stain marks found on slides exposed directly to air exhaled from the mouth. Duguid reported droplet diameters ranging from 1 to 2000 μm, with the majority being between 4 and 8 μm.

More recent studies agree that exhaled particles are mostly in the sub-micron size range, between 0.3 and 0.9 μm.[1,2,47–53] Studies that focus on particles that are emitted during sneezing and coughing give diameters between 1 and 16 μm.[54–56] Concentrations have been reported to range between about 0.001 and 2500 particles cm^{-3}, depending on the breathing method employed.[1,2,47,49,51–53,57] It appears that tidal breathing produces the lowest number of particles. As the tidal volume increases, so does the particle concentration.[2,49–52] The highest concentrations are generally produced during coughing or sneezing.[54,55,57] It has been observed that if inspiration is followed by a few seconds of breath hold, fewer particles are expired.[52,53] Moreover, large inter-individual variability in exhaled particle concentration has been observed,[1,2,47,48,50,52,53,56,57] as well as large intra-individual variability.[1,47,56]

Particle Formation Mechanisms

High air velocities in the airways associated with, e.g., sneezing and coughing have been shown to produce high numbers of particles.[54,55,57] During these types of activities, turbulence and dynamic compression of the airways cause shaking and vibrations of the airway walls, which in turn may produce droplets from the RTLF of primarily central airways.[58] The process is illustrated in Figure 4. Kleinstreuer et al.[59] pointed out that this type of turbulence-induced particle generation is unlikely to occur in the lower respiratory tract during normal breathing, since the airflow is laminar in the smaller bronchial airways down to and including the alveoli. The mechanism is therefore restricted to the larynx or perhaps to bifurcations, where local eddies can occur.

Another plausible mechanism for particle formation in human airways, associated with slow breathing, is based on the formation of film droplets. Recent work gives strong circumstantial evidence for such a mechanism in connection with airway closure and subsequent reopening.[47,48,50,53] After a deep exhalation, airway closure occurs. During inhalation and airway reopening, it has been proposed that a film of RTLF is spanned across the passage. When this film ruptures, droplets may form. The process is conceptually illustrated in Figure 5. The simplified and highly exaggerated figure gives an idea of film droplet formation after airway closure caused by compliant collapse, but film collapse would give a similar result.

Figure 4: Conceptual illustration of turbulence-induced particle formation in airways.

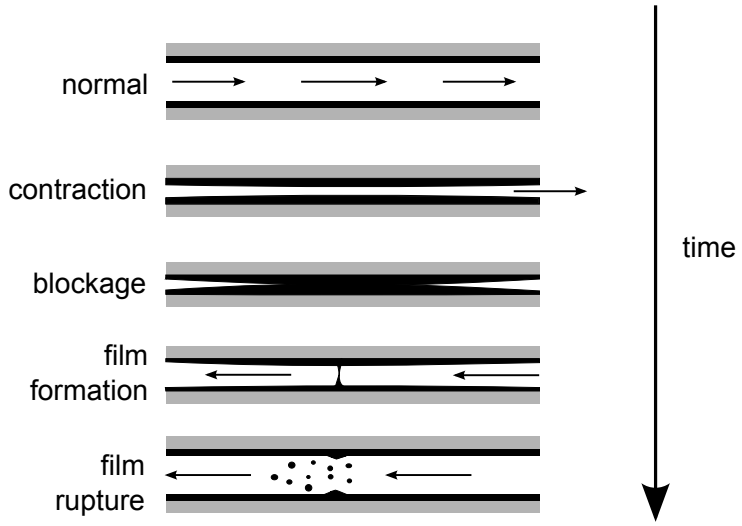

Figure 5: Conceptual illustration of film droplet formation in small airways. Exhalation is illustrated by arrows pointing to the right and inhalation by arrows pointing to the left.

Film Droplet Formation

The knowledge about film droplet formation stems mainly from studies of soap films and air bubbles in sea water. Blanchard[60] introduced the concept of film droplets in 1963, when he proposed that a bubble film in sea water begins to disintegrate by rupturing at a single point, and that the hole formed then rapidly widens. As the hole grows larger, it gathers film material along the rim of the hole in the form of a

toroid which subsequently breaks up into film droplets. The droplets cover a large size range and have considerable velocity in the direction of the advancing rim.[61] This means that droplets may impact in the vicinity of the outer edge of the film and be lost or cause formation of secondary splash droplets.[61,62] Formation of particles as small as 0.02 μm have been reported from bursting air bubbles at the sea surface.[63,64]

A flat soap film bursts by opening a hole driven by the surface tension of the fluid. Bursting is completed in a millisecond or less. As the film bursts, the equilibrium of surface tension forces in the plane of the film is broken, and the unbalanced forces at the edge of the hole set the liquid in motion. The liquid at the rim of the hole is exposed to extreme acceleration, and the velocity of the receding rim depends on the thickness of the film.[65] In vertical films, this usually varies with height. The rim of the hole does not remain smooth as it widens, since the accelerating film piles up at the edge of the rim and creates indentations at the tip. Ligaments form, which break and may leave the film as small droplets.[65,66]

Materials and Methods

Study Design

The general aim of the work performed in this thesis was to study the physical behaviour of exhaled aerosol particles, in order to shed some light on the underlying formation mechanism and the region of particle generation. Several experimental set-ups were developed and utilised. These are briefly described below, while more detailed information can be found in the appended papers. The commercial instruments that were used in the experiments are also introduced in this chapter.

Paper I

Number concentration and size are factors that largely determine the physical behaviour of exhaled particles. Moreover, the properties may provide information about where and how the particles are created. The specific aim of **Paper I** was to compare number size distributions from exhaled particles that were generated with different breathing techniques and from different individuals. The intention was to extend the knowledge about inter-individual variations and to contribute to the discussion on particle generation mechanisms and regions of formation.

Exhaled particles were sampled from sixteen healthy volunteers. The particles were generated from tidal breathing or from breathing reaching airway closure. In this study, tidal breathing meant that the subject, at rest, breathed normally into the instrument, without any control of volume or flow rate. For the airway closure manoeuvre, subjects were instructed to exhale slowly until no more air could be expired, reaching RV. This technique results in extensive airway closure. Exhaled particles were collected in a diffusion tight bag stored at 307 K in a thermostatted chamber. Number size distributions in the range from 0.01 to 2.0 μm were determined using an optical particle counter (OPC) and a scanning mobility particle sizer (SMPS) system, consisting of a differential mobility analyser (DMA) and a condensation particle counter (CPC). The set-up is illustrated in Figure 6.

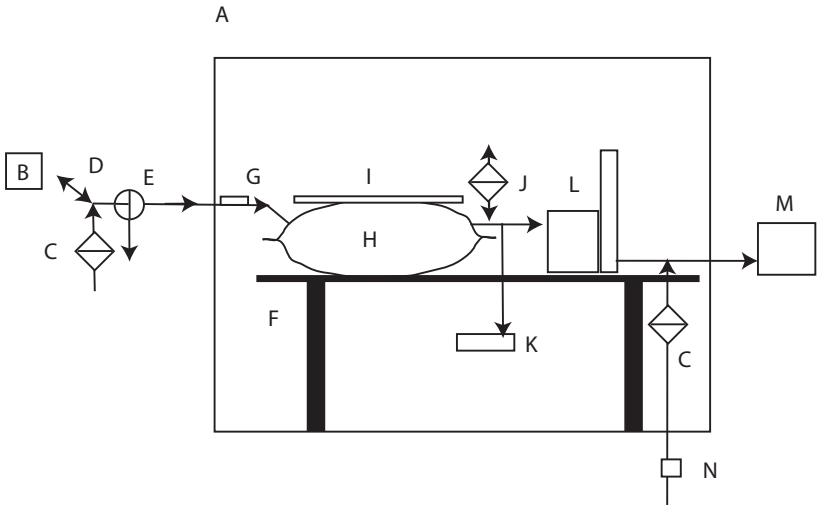

Figure 6: Set-up for studying number size distributions of exhaled particles in **Paper I**. The subject inhales particle-free clean air and exhales either into the surrounding air or into the apparatus. (A) thermostatted chamber (B) location of subject (C) high efficiency particulate air (HEPA) filter (D) automatic two-way non-rebreathing valve (E) manual two-way valve (F) table (G) ultrasonic flow meter to monitor exhalation flow rate (H) 30 litre diffusion-tight storage bag (I) pressure plate to apply constant pressure over the sampling bag (J) two-way HEPA filter (K) optical particle counter (OPC) (L) differential mobility analyser (DMA) (M) condensation particle counter (CPC) (N) mass flow controller for dry air.

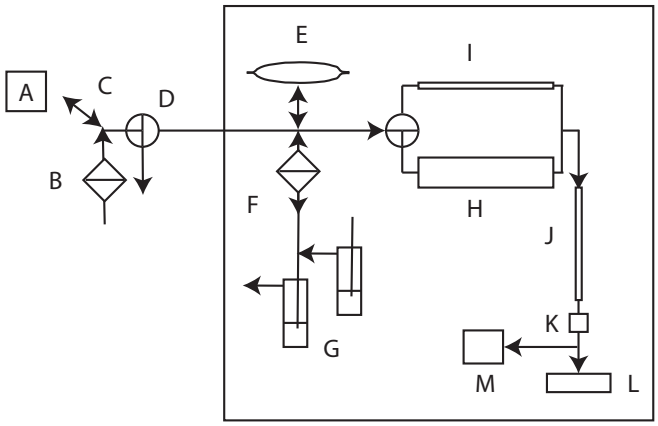

Figure 7: Set-up for studying number size distributions of exhaled particles at various relative humidities in **Paper II**. The set-up is located in a climate chamber, and the subject inhales particle-free clean air and exhales either into the surrounding air or into the apparatus. (A) location of subject (B) high efficiency particulate air (HEPA) filter (C) automatic two-way non-rebreathing valve (D) manual two-way valve (E) buffer bag (F) two-way HEPA filter (G) water locks, allowing excess air to escape when the buffer bag is filled to capacity and filtered air to enter the system to avoid choking the instrument pumps when the bag is empty (H) diffusion drier (I) copper tube (J) oven (K) dew point meter (L) optical particle counter (OPC) (M) pump for regulating total flow in set-up.

Paper II

The equilibrium diameter of an aqueous droplet containing non-volatile substances varies with relative humidity (RH). When endogenously produced particles are exhaled, they usually enter an environment where the RH is lower than in the respiratory tract. The particles are then expected to shrink due to evaporation of water. The scope of **Paper II** was to evaluate the relation between humidity and size of exhaled particles, in order to gain knowledge of the number size distribution at the point of particle generation. This will aid the understanding of the underlying formation mechanism. Further, particle size is an important factor when investigating, e.g., life time in air as well as choice and efficiency of collection methods.

Number size distributions of exhaled particles were measured at easily controlled RHs, and subsequently extrapolated to the range of interest, i.e., inside the human lung. Breathing reaching airway closure, as described in **Paper I**, was employed. Three subjects volunteered for the study. The set-up, illustrated in Figure 7, was similar to that in **Paper I**, but with ovens and diffusion driers added to control temperature and humidity of the exhaled air. Three different measurement modes were used. In all modes, the chamber temperature was set to 308 K. In the first mode, particles were measured without interfering with humidity. In the second mode, exhaled air and particles were dried in a diffusion drier. Particles were expected to shrink due to evaporation of water. In the third mode, exhaled air was directed through a diffusion drier and subsequently through an oven set to 348 or 423 K. The intention was to drive off as much as possible of the remaining water from the particles, causing a phase transition and further size reduction. Particles were measured with an OPC.

Paper III

Exhaled particles may be collected and sampled for chemical analysis, but the small amount of material available necessitates a very effective sampling procedure. It is therefore desirable to find ways to maximise the amount of expired particles without putting undue requirements on the subject under study. The specific aim of **Paper III** was to investigate how a short breath hold at functional residual capacity (FRC), residual volume (RV) or total lung capacity (TLC) influences the concentration and size distribution of exhaled particles. The findings will help improve the efficiency of exhaled particle collection, and furthermore aid the understanding of particle formation mechanisms and related processes.

Number size distributions of exhaled particles were measured after well-defined periods of breath hold, either at FRC (FRC manoeuvres), RV (RV manoeuvres) or at TLC (TLC manoeuvres). Breath hold at TLC was preceded by exhalation to RV. Particles were measured with an OPC, and nineteen healthy subjects participated in

the study. The experimental set-up is described in detail by Almstrand et al.[1], and is illustrated in Figure 8. Specific to this study is an ultra-sonic flow meter at the mouth end, which makes it possible to record and visualise both inhalation and exhalation flow rate in real time, thus enabling compliance to the prescribed manoeuvre. Expiratory flow rates were kept low in order to avoid dynamic compression, which may result in exhaled particles from large airways.[46] The set-up was housed at 309 K to avoid condensation in the equipment.

For breath hold at TLC, it is likely that a size dependent fraction of the particles generated in small airways settle in the alveoli. Some deposition is also expected in the bronchioles. A rough estimate of deposition loss can be made from particle size and alveolar dimensions. In the present study, an alveolus was approximated by a spherical volume with a diameter of 0.3 mm and two idealised situations for gravitational settling were modelled. The first model describes settling in well-mixed air, and the other settling in still air. Diffusion may also be a cause of particle loss in the respiratory system, but this process becomes important when the particles are smaller than 0.5 μm.[14] The instrument used here can only detect particles larger than 0.41 μm, and diffusion was therefore not considered in any of the models. Impaction is a source of loss mainly for large particles in large and medium-sized airways,[14] and was not considered either. Interception was not taken into account, since the likelihood of interception in the airways would depend on the proximity of the gas streamline to the airway surface and on the ratio of particle size to airway diameter. These factors are usually small even in the smallest airways.[14]

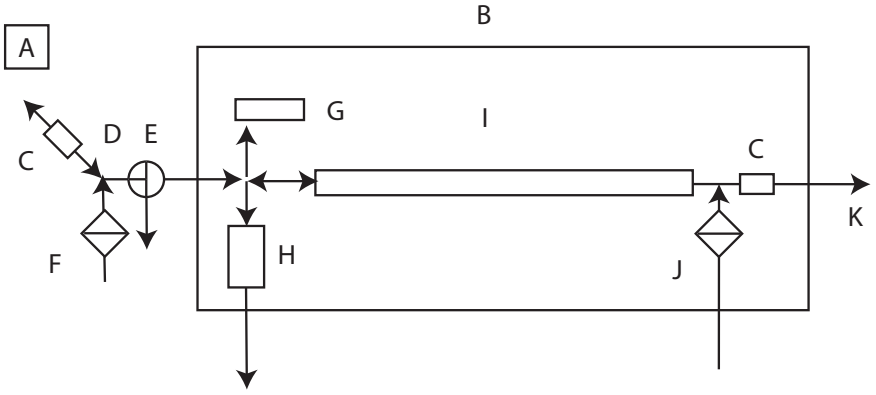

Figure 8: Set-up for studying the effect of breath hold on amount of exhaled particles in **Paper III**. The set-up is located in a climate chamber, and the subject inhales particle-free clean air and exhales either into the surrounding air or into the apparatus. (A) subject under investigation (B) thermostatted box (C) ultrasonic flow meter to monitor and control breathing patterns (D) automatic two-way non-rebreathing valve (E) manual two-way valve (F) high efficiency particulate air (HEPA) filter (G) optical particle counter (OPC) (H) impactor with associated flow meter and pump (samples were not analysed in this study) (I) tubular reservoir (J) moist air added at a rate slightly exceeding the rate of extraction by the OPC and impactor (K) vent.

Paper IV

Aerosol particles may be generated from rupturing liquid films. The formation process, connecting film properties to droplet number and size, has received little attention. The work performed in **Paper IV** was undertaken with the aim to understand the influence of film dimensions on droplet formation, with possible implications for exhaled particles. An additional goal was to investigate the effect of surface tension on film droplet formation.

The film droplet formation mechanism, which is likely to be the mechanism responsible for particle formation in small airways, was experimentally mimicked by using a purpose-built instrument, shown in Figure 9. Working fluids with various surface tension were spanned across holes of different diameter and length, i.e., across perforated plates, each with well-defined hole diameters and of known thickness. As the films burst, droplets were formed. The total droplet concentrations were measured with a CPC, while number size distributions were measured with an OPC. The number of droplets generated from a plate was calculated by summing the product of the concentrations given by the instruments with the flow rate through the chamber and the averaging time for the concentration measurement. This quantity was divided by the number of holes in the plate and the surface area of one hole to give the number of droplets formed per unit surface area of film and is referred to as specific droplet formation capacity (SDFC). Furthermore, an average droplet diameter was calculated for each film diameter and working fluid.

The diameter of the holes in which the fluid films were spanned ranged from 0.95 to 8 mm. The thickness of the perforated plates varied between 0.1 and 1.45 mm. Arranged in the order of increasing surface tension, the working fluids used were phosphatidylcholine (PC) solution, sodium dodecyl sulphate (SDS) solution, diluted Curosurf®, PC/protein mix and isotonic NaCl solution. Some fluids were chosen to illuminate the effects of properties such as surfactant solubility and surface tension on the film droplet formation process, while others were selected since they contain constituents that have been found in RTLF. This is described in more detail in the appended paper.

Unpublished Work

In an attempt to further explore exhaled particles, they were collected and imaged in a scanning electron microscope (SEM). Breathing reaching airway closure was employed, and collection took place in the experimental set-up described by Almstrand et al.[1] and in Figure 8. Briefly, particles were collected on a silicon plate, using a cascade impactor. Particles were imaged under high vacuum conditions.

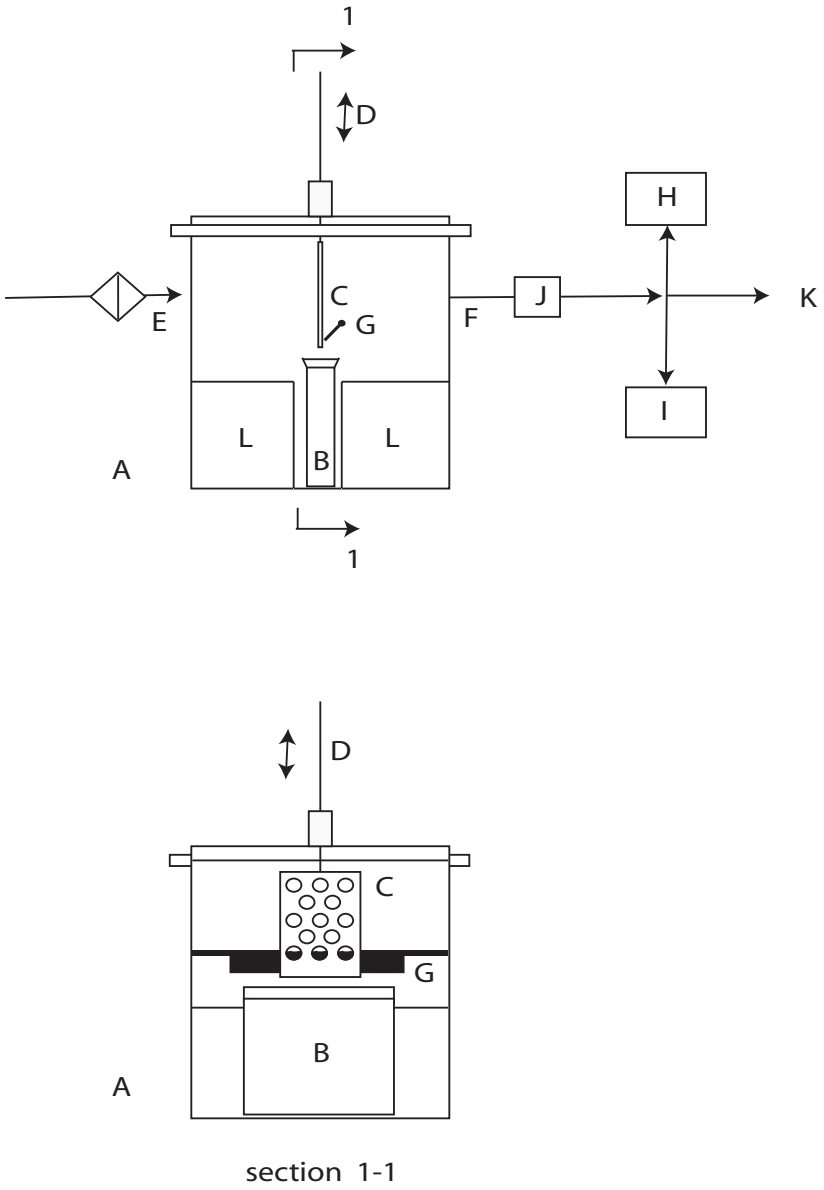

Figure 9: Set-up for studying film droplet formation in **Paper IV**. The bottom illustration is a section through the top illustration, viewed in the direction of the section arrows. (A) air-tight chamber (B) working fluid container (C) exchangeable perforated plate (D) movable rod to manually extract from, or immerse plate in working fluid (E) filtered nitrogen gas inlet (F) particulate-laden nitrogen gas outlet (G) scraper to remove excess liquid from perforated plate (H) optical particle counter (OPC) (I) condensation particle counter (CPC) (J) dew point meter (K) vent (L) sealed-off volume.

Instrumentation

Optical Particle Counter (OPC)

The optical particle counter (OPC) used in **Paper I-IV** was a Grimm dust monitor 1.108 (Grimm Aerosol Technik GmbH, Ainring, Germany). This instrument measures size distributions of particles by means of single particle light scattering. A laser source is used to illuminate the particle as it passes through a detection chamber (see Figure 10). As the particle passes through a laser beam, light is scattered. The scattered light is collected by a concave mirror at scattering angles ranging from 60 to 90 degrees, and reflected onto a photodiode. After current/voltage conversion and proper amplification, the signal of the diode passes a multi-channel size classifier. The number of pulses together with the flow rate gives the particle count, and pulse height gives the particle size.

In **Paper I**, **II** and **IV**, the instrument was operated in a 6 second averaging mode, and delivered concentration data in fifteen size intervals, formally from 0.3 to greater than 20 μm. In **Paper III**, it was operated in a 1 second averaging mode, with eight size intervals measuring particles in the range from 0.3 to greater than 2.0 μm. The instrument is calibrated using NIST-traceable polystyrene latex spheres. The optical properties of latex spheres are quite different from those of exhaled particles, which are assumed to contain mostly water. In **Paper I**, Mie-theory was applied to perform a correction of the size interval limits to better represent the actual physical dimensions of aqueous droplets. The adjusted size intervals are found in Table 2. These corrections were utilised also in **Paper III**, but not in **Paper II** or **Paper IV**. The reason for not applying the calculations in **Paper II** is that the particles there were dried and heated prior to analysis. Hence, it is not reasonable to assume that they can be approximated by liquid water droplets. In **Paper IV**, the particles were not exhaled particles, but droplets containing several different solutes.

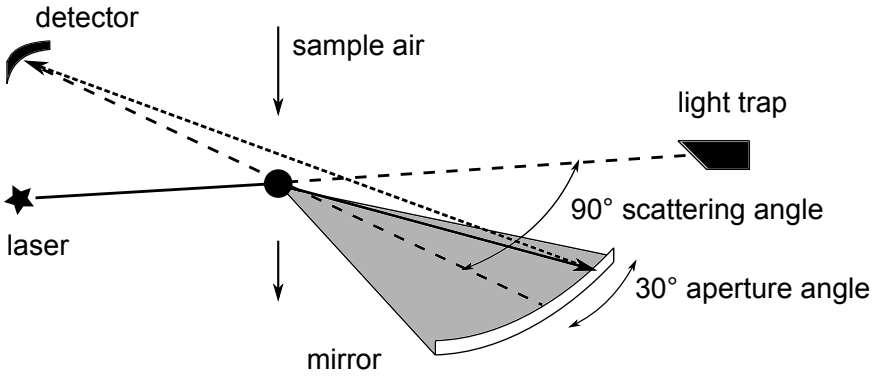

Figure 10: Working principle of the Grimm dust monitor (obtained and adapted from http://www.dustmonitor.com, courtesy of Grimm Aerosol Technik GmbH).

Table 2: Original and adjusted interval limits for the Grimm dust monitor.

original interval (μm)	adjusted interval (μm)
0.3-0.4	0.41-0.55
0.4-0.5	0.55-0.70
0.5-0.65	0.70-0.92
0.65-0.8	0.92-1.14
0.8-1.0	1.14-1.44
1.0-1.6	1.44-2.36
1.6-2.0	2.36-2.98
2.0-3.0	2.98-4.55
3.0-4.0	4.55-6.15
4.0-5.0	6.15-7.77
5.0-7.5	7.77-11.9
7.5-10	11.9-16.1
10-15	16.1-24.5
15-20	24.5-33.1
>20	>33.1

Differential Mobility Analyser (DMA)

In **Paper I**, exhaled particles were sorted according to size using a differential mobility analyser (TSI DMA 3071, TSI Inc., Shoreview, MN, USA). The instrument, illustrated in Figure 11, classifies aerosol particles according to their electrical mobility. The method is independent of other particle properties, such as density. The first step in the DMA technique is to neutralise the incoming aerosol to ensure a predictable distribution of charges amongst the particles. The aerosol sample is therefore passed through a radioactive bipolar charger, by which a bipolar equilibrium charge is established. This way, an equilibrium state is obtained, with known fractions of particles carrying no charge, single charge or multiple charges (positive or negative). The fraction of particles carrying zero charge increases with decreasing particle diameter. In fact, 99.32% of all particles with diameter 0.1 μm will carry zero charge.[67] Following charging, the particles are injected into the DMA, where they are allowed to migrate into a laminar flow of particle-free air (sheath air). The DMA consists of a hollow, earthed cylinder with a concentric rod in the middle. The rod is connected to a negative power supply that provides a negative potential and creates an electric field inside the instrument. This field influences the flow trajectory of the incoming particles. A negatively charged particle is repelled towards and deposited on the inner wall of the DMA and a particle with neutral charge exits the instrument with the sheath air. A particle with positive charge will move towards the negatively charged central rod. This particle will be accelerated until it reaches a certain constant limiting velocity, which depends on the magnitude of the electric field and on the electrical mobility and charge of the particle. For spherical particles, the electrical mobility is inversely related to particle size. If all particles have the

same charge, then all particles of a given mobility will be of the same size. Particles within a narrow range of electrical mobility achieve just the right velocity to be able to exit the DMA through a sample slit. Particles with greater mobility migrate to the central rod before reaching the slit, while those with lower mobility go beyond the slit and are extracted out. Adjusting the magnitude of the electric field inside the DMA controls the size of the exiting particles.

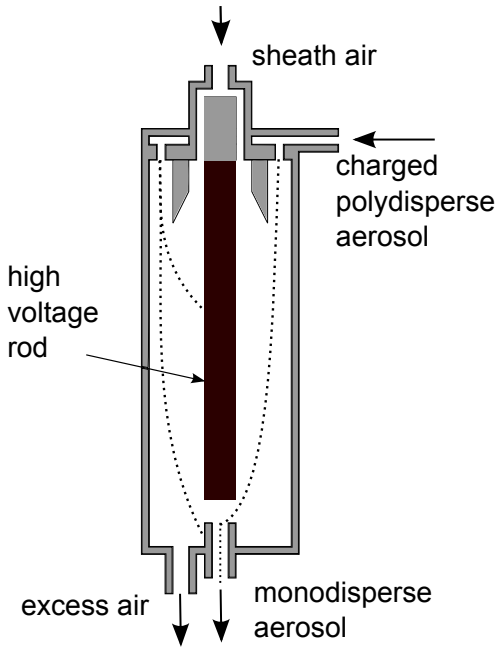

Figure 11: Differential mobility analyser (DMA).

Condensation Particle Counter (CPC)

In **Paper I** and **Paper IV**, number concentrations of particles larger than 0.01 μm were measured with a condensation particle counter (TSI CPC 3022 or TSI CPC 3010, TSI Inc., Shoreview, MN, USA), illustrated in Figure 12. A CPC operates like an OPC, in which particles are detected by light scattering. In a CPC, however, a condensing vapour enlarges the particles before they are counted. This enables detection of particles that are normally too small to be detected by optical methods, i.e., particles that are too small to scatter sufficient amounts of light. The instrument operates by drawing an aerosol sample through a heated saturator, in which a working fluid (normally n-butanol) is vaporised and diffuses into the sample stream. The aerosol sample becomes saturated with the vapour from the working fluid and then continues into a cooled condenser. Inside the condenser, the vapour becomes supersaturated. When sufficient supersaturation is reached, the vapour begins to condense on the particles. Once condensation begins, the particles quickly grow into larger liquid droplets. The enlarged particles are detected and counted by light scattering. Light scattered by an individual particle is recorded as a voltage pulse.

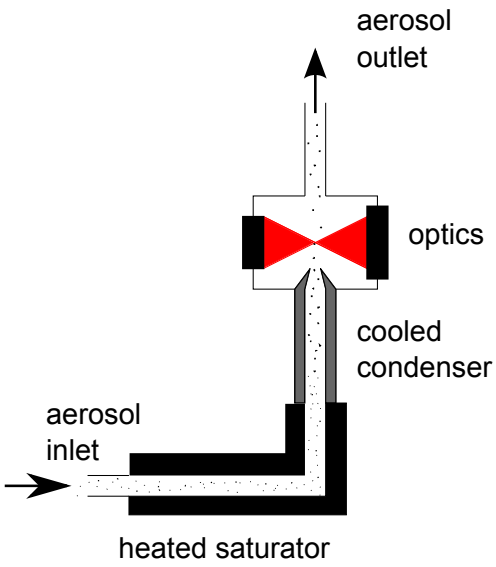

Figure 12: Condensation particle counter (CPC).

Scanning Mobility Particle Sizer (SMPS)

In **Paper I**, a scanning mobility particle sizer (TSI SMPS 3936, TSI Inc., Shoreview, MN, USA) system was used to measure number size distributions of exhaled particles in the range from 0.01 to 0.43 μm. An SMPS system contains a DMA and a CPC. The DMA is scanned over a range of sizes by varying the applied electric field, and the particle concentration for each mobility range is measured with the CPC. The drawback of the SMPS system is that it only observes charged particles in a small interval of the size distribution at any given time. This makes statistically sound measurements quite time consuming if concentrations are low. When studying exhaled particles, the measurement procedure becomes impractical from a breathing subject's point of view.

Dew Point Meter

Dew point meters were used in **Paper II** (Optidew High Performance Optical Dew-Point Transmitter, Michell Instruments, Ely, UK) and **Paper IV** (System 1100 DP Hygrometer, General Eastern Industries, USA) to track relative humidity (RH) during the experiments. The essential part of a dew point meter is a cooled, polished metal mirror. At a certain temperature, and for a constant barometric pressure, the water vapour in air that is passed over this mirror will condense into liquid water. The liquid water is fogging the mirror and reducing its reflection, thus indicating the dew point. The dew point is found at saturation temperature, and is associated with RH. At 100% RH, the dew point is equal to the current temperature, and the air is maximally saturated with water.

Ultrasonic Flow Meter

An ultrasonic flow meter (OEM Flow Sensor Spiroson-AS, ndd Medical Technologies, Zürich, Switzerland) was used in **Paper I** and **Paper III** to provide information on inhalation and exhalation flow rates during the experiments. The instrument measures the velocity of a gas by ultrasound. More specifically, it measures the difference in transit time of ultrasonic pulses propagating in and against the direction of the flow. This gives the average velocity of the gas along the path of the ultrasonic beam. The ultrasonic flow meter used here measures gas flows at 200 Hz.

Cascade Impactor

In the unpublished work, a modified commercial three-stage cascade impactor (PM10 Impactor, Dekati Ltd, Tampere, Finland) was used to collect exhaled particles. A cascade impactor is normally used to classify aerosol particles according to size and to collect them on impaction plates for subsequent analysis. The aerosol under investigation is drawn into the impactor via a nozzle or jet, and travels through a series of orifices of decreasing size. This is illustrated in Figure 13. The output stream after each stage in the impactor is directed against an impaction plate. Particles with sufficient inertia cannot follow the streamlines, but will impact on the flat plate. Smaller particles are able to follow the streamlines and will continue to the next stage in the impactor. Here, the nozzle is smaller and the velocity through the nozzle is higher, causing smaller particles to impact on the plate. Thus, particles are separated stepwise by their momentum differences into a number of size ranges. The impactor used in this work had three stages, but particles were only collected on the last stage, i.e., in the range 0.5-2.0 μm. The collection surface was a silicon plate.

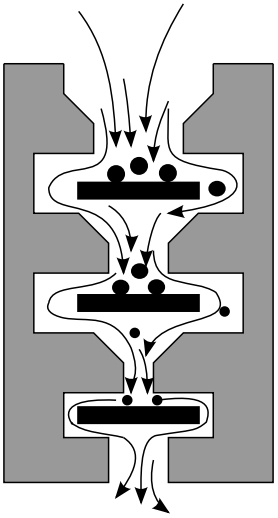

Figure 13: Cascade impactor.

Scanning Electron Microscope (SEM)

Exhaled particles that were collected by impaction in the unpublished work were imaged using a scanning electron microscope (LEO 1550 FEG SEM, Ångström Scientific Inc., Ramsey, NJ, USA). A SEM is a microscope that uses electrons rather than light to produce an image. A focused electron beam scans a sample and secondary electrons are produced. These electrons are collected by a positively charged detector, and converted to an electric signal. The number of secondary electrons emitted and reaching the detector depends on the topography of the sample. SEM analysis is considered non-destructive, making it possible to analyse the same sample repeatedly.

Results

Number Size Distribution of Exhaled Particles in the Range from 0.01 to 2.0 μm

Number size distributions of particles generated from tidal breathing and from breathing reaching airway closure were measured for sixteen healthy subjects in **Paper I**. Two groups of individuals could be identified; high emitters and low emitters. During tidal breathing, the low emitters (n=14) exhaled less than 10 particles cm^{-3} while the high emitters (n=2) reached levels of more than 50 particles cm^{-3}. When breathing reaching airway closure, low emitters (n=14) exhaled less than 30 particles cm^{-3}, and high emitters (n=2) again as much as 50 particles cm^{-3}. Statistical characteristics for all exhaled particle concentrations are shown in Table 3, while detailed data on individuals are found in the appended paper. No relation was found between particle concentration and lung function, age or gender. Moreover, there was no correlation between the total number of particles emitted from a subject when breathing tidally and when breathing reaching airway closure. A subject who emitted high concentrations of particles during tidal breathing did not necessarily do so when breathing reaching airway closure.

Table 3: Statistical characteristics of exhaled particle concentrations from all subjects, i.e., including both high and low emitters (n=16). The scanning mobility particle sizer (SMPS) measured particles in the range from 0.01 to 0.43 μm, and the optical particle sizer (OPC) from 0.41 to 33 μm.

		average conc. (cm^{-3})	standard dev. (cm^{-3})	maximum conc. (cm^{-3})	median conc. (cm^{-3})	minimum conc. (cm^{-3})
Tidal breathing	SMPS	10.8	22.3	82.7	3.1	0.6
	OPC	0.06	0.06	0.23	0.03	0.02
Airway closure	SMPS	16.9	17.3	68.9	12.2	3.9
	OPC	5.3	3.5	12.1	3.9	1.0

The individual number concentrations achieved from breathing reaching airway closure were in all but two cases higher than the concentrations achieved from tidal breathing. In these two cases, the number of particles generated during tidal breathing was a factor 16 and 27 higher than the average value of the other fourteen subjects. The fact that the two subjects were non-European has no significance here, but may warrant closer investigation in the future.

Average number size distributions for tidal breathing and for breathing reaching airway closure are illustrated in Figure 14. High emitters are not included in the figure, since they would dominate the distribution function and hide the typical average values for the remaining individuals. However, the distributions peak at the same diameter both with and without high emitters included. During tidal breathing, there is a single mode at around 0.07 μm. When switching to breathing reaching airway closure, this mode remains, but an additional, stronger mode is found between about 0.2 and 0.5 μm. No particles larger than 4.55 μm were detected.

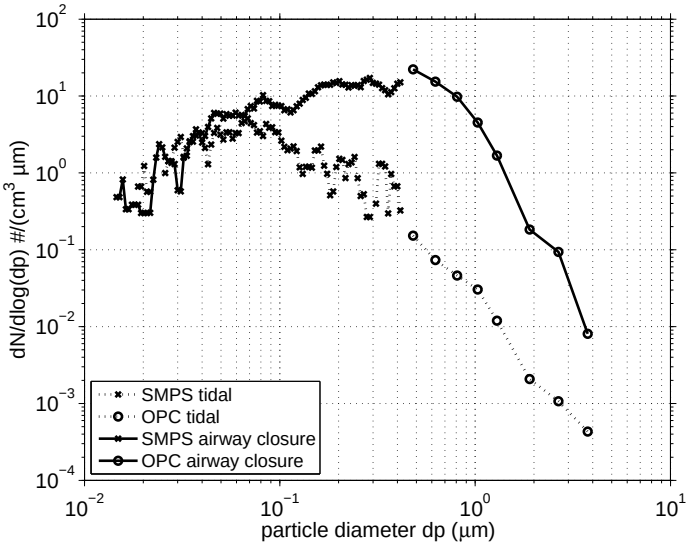

Figure 14: Particle number size distributions obtained in **Paper I**. Average for all participating low emitters. Data are positioned at the mid-diameter of each interval.

Relation Between Humidity and Size of Exhaled Particles

Number size distributions of exhaled particles were measured at a relative humidity (RH) of between 5.2 and 84.8% in **Paper II**. The total concentration of particles appeared to decrease as the humid exhaled air was sent through a diffusion drier, lowering the RH to between 5 and 28%. In experiments where the particles first were dried and then subsequently heated, the OPC reported increased concentrations. Detailed data on the experiments are found in the appended paper. In all

measurements, the number size distribution peaked in the smallest interval of the OPC; hence a smaller or larger fraction of the distribution was not measured. Attempts were made to also use an SMPS system in the set-up, but with total counts of between 20 and 100 particles during a 20 minute measurement period, it became evident that the total scanning time was too short to provide reliable size distributions. Longer measurement periods were not practical from the breathing subject's point of view.

The location of the obtained size distributions required unusual data assessment. Experimental data were evaluated under the assumption that the size distribution function between 0.3 and 0.4 μm (the smallest size interval of the OPC) was constant across the interval. It was also assumed that all particles in the distribution change volume by a constant factor upon a change in RH in the surrounding air. The volume change gives rise to a diameter change, which can be expressed in terms of the apparent decrease in particle concentration caused by the distribution shifting over the lower detection limit of the OPC. Further, a simple model based on Raoult's law was set up to theoretically describe the volume of a liquid particle as a function of RH. A relation between particle volume and RH was fitted to experimental data, and extrapolated to 99.5% RH. The calculations are described in detail in the appended paper, and the results show that exhaled particles shrink by a factor of approximately 0.42 when they leave the saturated environment inside the human body for a surrounding with 75% RH. This is illustrated in Figure 15, where the measured size distribution is compared to the distribution that is expected at 99.5% RH, i.e., inside the human lung where the particles are generated.[68]

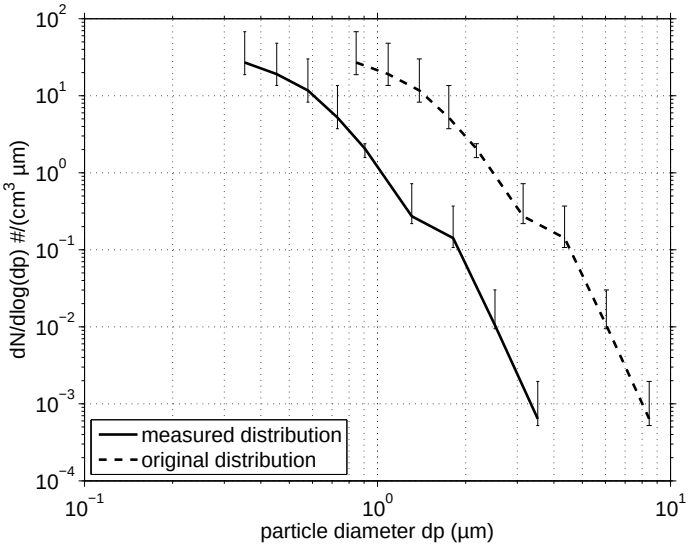

Figure 15: Shift in particle number size distribution caused by a change in relative humidity (RH). The solid line represents the particles at 75% RH and the dashed line shows the expected original distribution at 99.5% RH. The figure also illustrates the minimum and maximum values for individual experiments.

Effects of Breath Holding at Low and High Lung Volumes on Amount of Exhaled Particles

In **Paper III**, number size distributions of exhaled particles were measured after short periods of breath hold at FRC, RV or TLC. Breath hold at RV resulted in successively increased particle number concentration with time. After 5 and 10 seconds breath hold, the median concentration increased by 63% and 110%, respectively. Breath hold at FRC resulted in an increased particle concentration after 5 seconds, but additional breath hold time did not cause any further increase. After 10 seconds breath hold, the median concentration was 88% higher than that obtained at no breath hold. On average, the RV manoeuvre resulted in about four times higher particle concentration than the FRC manoeuvre. Breath hold at TLC caused a successive decrease in particle concentration with time. After 5 seconds breath hold at TLC, the median concentration decreased by 43%, while 10 and 20 seconds breath hold resulted in a loss of 58% and 75% of the particles, respectively. Median values are shown in Figure 16, where p-values are included. Both inter- and intra-individual variations were large. The highest individual particle concentration was 34 times higher than the lowest at no breath hold at RV, 21 times at FRC and 22 times at TLC. The coefficient of variation (CoV) within individuals varied between 0 and 99%.

Particle number size distributions following the FRC and RV manoeuvres are shown in Figure 17A and 17B, illustrating the considerably higher concentrations obtained from the RV manoeuvre. Also shown, in Figure 17C, are the point by point ratios between data from the FRC manoeuvre and the RV manoeuvre. If the same mechanism is responsible for the particle generation in both manoeuvres, the ratio is expected to be constant over all sizes for a given breath holding time. This is approximately the case for particles smaller than about 1 μm.

Particle number size distributions for breath hold at TLC are compared to that of no breath hold in Figure 18A. Also illustrated is a comparison between the observed concentrations and the concentrations predicted by the models described in the Materials and Methods section and in the appended paper. Figure 18B shows the point by point ratios between the concentrations predicted by the well-mixed air deposition model and the observed concentration. Figure 18C shows the corresponding ratios for the still air deposition model. A full agreement between observation and model would give values of 1.0 throughout. Here, however, it is clear that the observed decrease is considerably larger than the calculated decrease, averaged over all particle sizes.

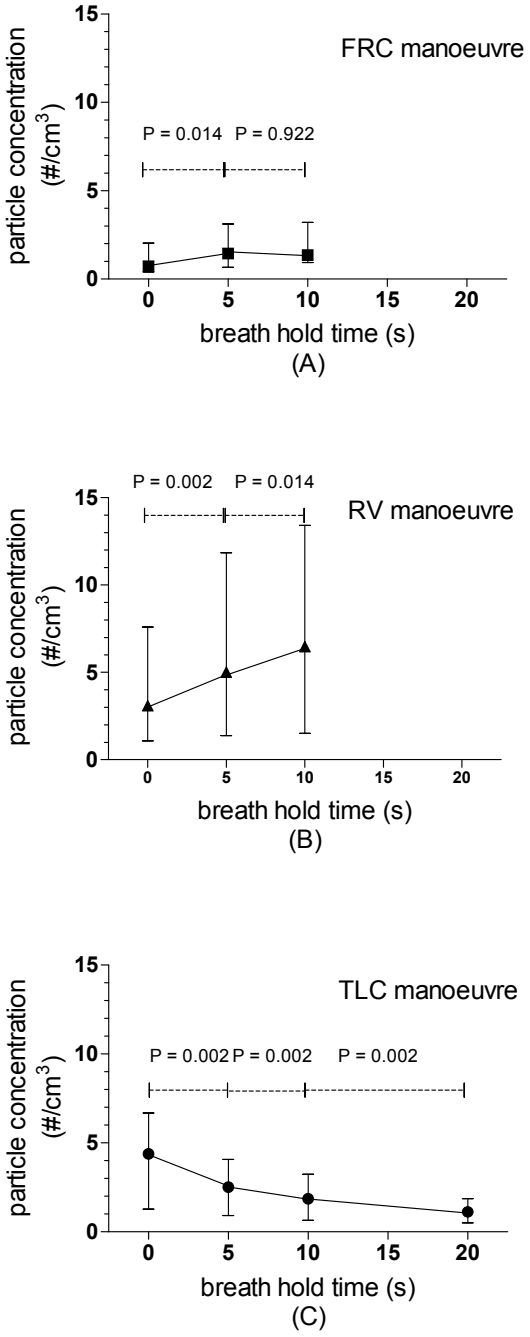

Figure 16: Median particle concentration versus breath holding time for the (A) FRC manoeuvre (B) RV manoeuvre and (C) TLC manoeuvre. The vertical bars refer to 25-75 percentiles. P-values are two-tailed and according to Wilcoxon matched pairs test.

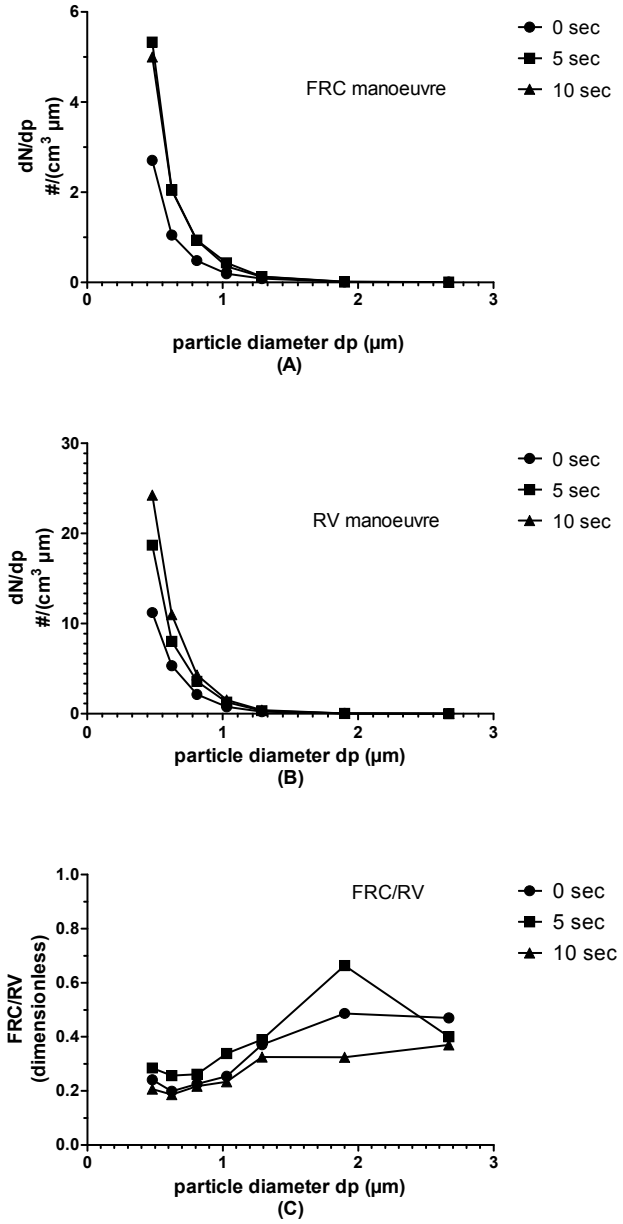

Figure 17: Number size distribution of particles obtained after breath hold at (A) FRC and (B) RV. (C) shows the point by point ratios between values obtained from the FRC manoeuvre and the RV manoeuvre.

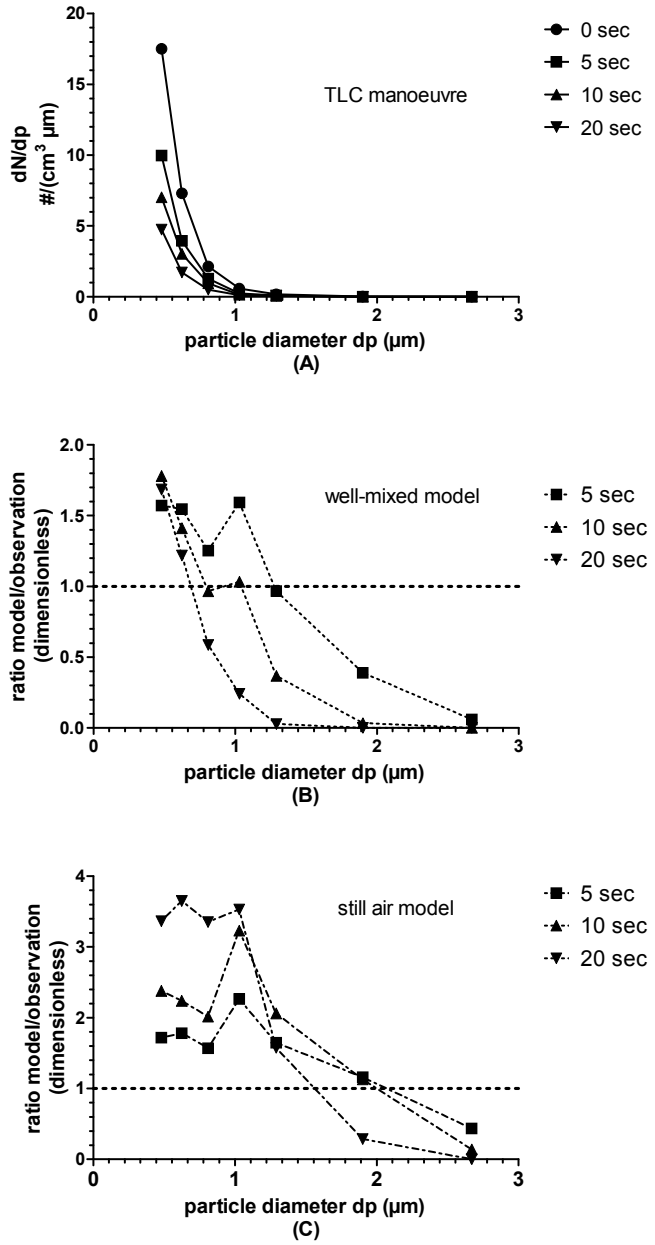

Figure 18: Particle number size distributions obtained after breath hold at TLC. (A) shows the measured distributions. (B) shows the point by point ratios between the values obtained from the model describing gravitational settling in well-mixed air and the observed values. (C) shows the point by point ratios between the values obtained from the model describing gravitational settling in still air and the observed values. The dotted horizontal lines indicate the ideal ratio 1.0, where observation and model would be in full agreement.

Influence of Film Dimensions on Film Droplet Formation

In **Paper IV**, the film droplet formation process was experimentally mimicked in a purpose-built instrument, and the specific droplet formation capacity (SDFC) and average droplet diameter were calculated. Numbers and sizes did not vary much, even though working fluids with no, insoluble and soluble surfactants were used in the experiments. Average values for each working fluid are found in Table 4. SDFC drops with decreasing surface tension for all working fluids except the PC/protein mix. Droplet diameter is not related to surface tension.

SDFC obtained from each working fluid and film diameter are illustrated in Figure 19. Values ranged between 0 and 20, but rarely exceeded 5 droplets mm^{-2}. No general relation was found between film dimension and SDFC, and there was no trend towards reduced SDFC with reduced film diameter. Another observation was that thick plates generally gave fewer droplets than did thin ones. Again, the PC/protein mix deviates from the pattern. Figure 20 shows the resulting droplet diameter for each working fluid and film diameter. Standard deviations are large, but it seems like the smallest droplets were generally created from the smallest fluid films.

Table 4: Specific droplet formation capacity (SDFC) and resulting droplet diameter for each working fluid, averaged over all film diameters, i.e., all plates. Standard deviations (SD) are included. The table also gives the surface tension of the working fluids.

working fluid	surface tension ($mN\ m^{-1}$)	SDFC average±SD (mm^{-2})	droplet diameter average±SD (μm)
Isotonic NaCl solution	75	2.41±1.88	0.42±0.14
PC solution	29	0.22±0.14	0.33±0.16
PC/protein mix	50	0.39±0.61	0.19±0.07
SDS solution	37	1.33±1.05	0.49±0.27
Diluted Curosurf ®	39	0.57±0.68	0.31±0.10

Images of Exhaled Particles

Exhaled particles were collected on silicon plates using a cascade impactor and subsequently imaged by a SEM. In Figure 21, objects collected in the middle of the plate appear to be 10-15 μm in diameter, but smaller objects are seen in the periphery of the plate. Figure 22 is a magnification of an edge of Figure 21. Here, single objects in the sub-micron size range are clearly visible.

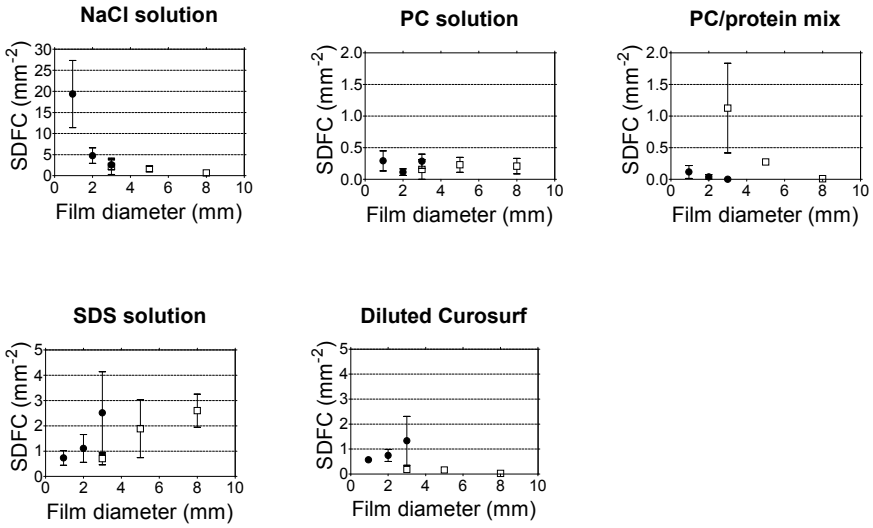

Figure 19: Specific droplet formation capacity (SDFC). The number of droplets generated per mm^2 of available film. • represent thin plates (0.1 mm) and □ thick plates (0.95-1.45 mm). The error bars denote the standard deviation of the average values.

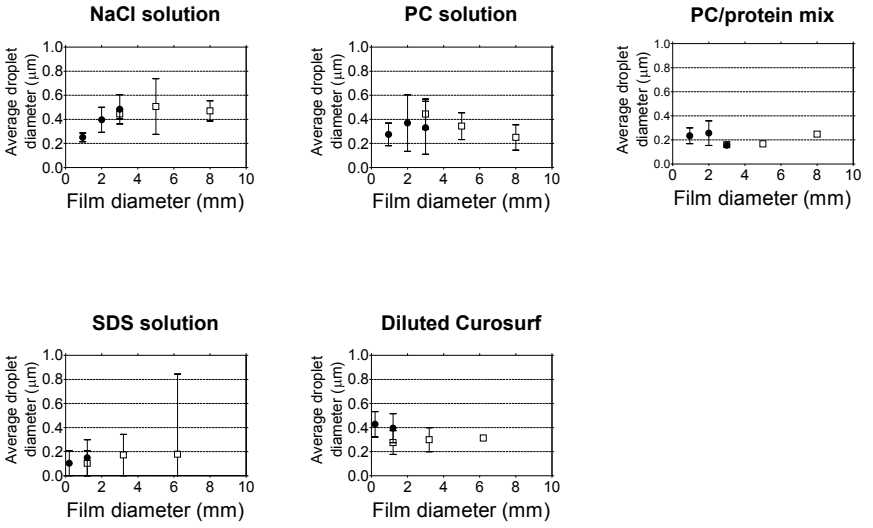

Figure 20: Average droplet diameter. • represent thin plates (0.1 mm) and □ thick plates (0.95-1.45 mm). The error bars denote the standard deviation of the average values.

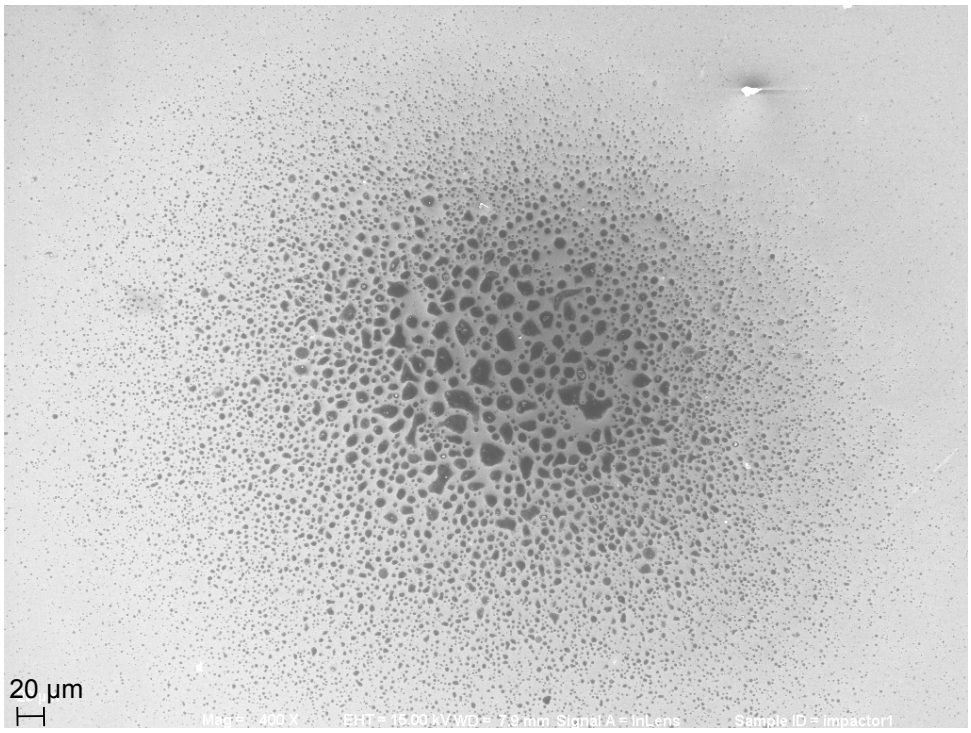

Figure 21: Exhaled particles collected through an impactor on a silicon plate, and imaged by a scanning electron microscope (SEM).

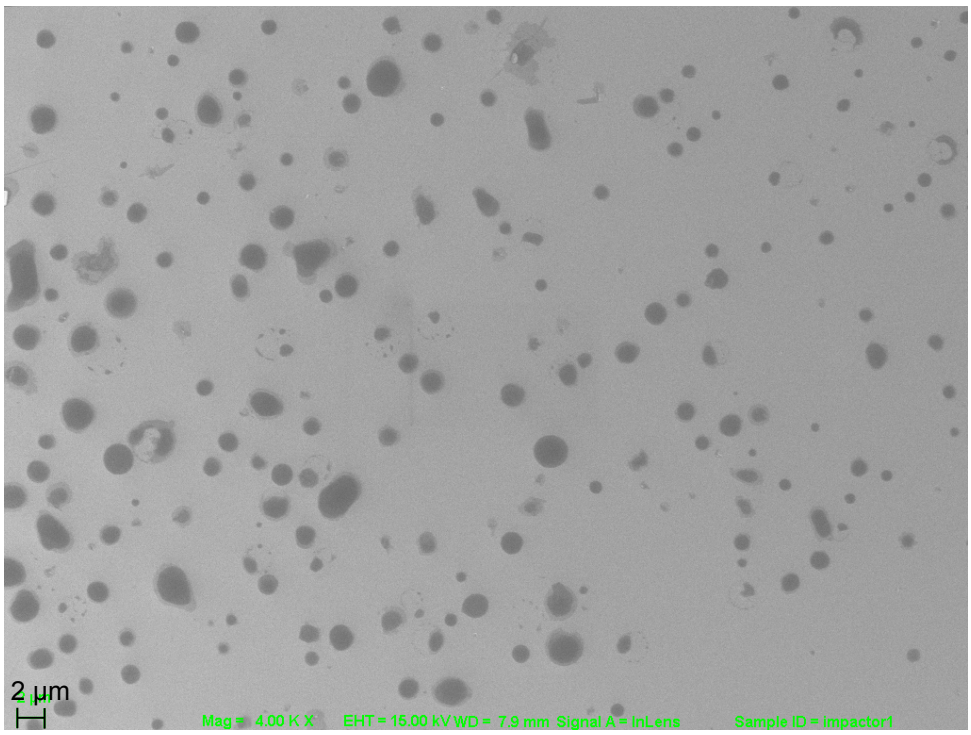

Figure 22: Exhaled particles collected through an impactor on a silicon plate, and imaged by a scanning electron microscope (SEM). Magnification of Figure 21.

Discussion

Inter-Individual Variability

Particles exhaled by a total of 28 healthy individuals (14 male, 14 female, ages 25-70) were measured throughout **Paper I-III**. It is clear that the inter-individual variation in concentration is very high, while the number size distribution appears to be similar for all subjects. The variability may be due to differences in lung structure between individuals. For example, airway closure, which is considered the mechanism responsible for film droplet formation, can occur at different generations of the airways also for healthy individuals.[29,32] Moreover, although no obvious relation between exhaled particle concentration and subject age was found in this work, previous studies have shown an age related increase.[50,53,54] This increase can be explained by the observation that elderly subjects reach airway closure at an earlier stage of exhalation than younger individuals.[29,32,34] Gebhart et al.[52] do not mention an age related increase, but simply conclude that subjects with collapsing peripheral airways have an increased production rate of particles. This argument appears reasonable and the absence of a relation between particle concentration and subject age in this work may be explained by the fact that the majority of subjects studied were in the same age range, between 30 and 40 years.

It has been suggested that variations in the composition of RTLF account for the inter-individual variations in exhaled particle concentration, but the results are somewhat contradictory. Edwards et al.[57] and Watanabe et al.[69] agree that saline delivery to the lungs can diminish the number of particles emitted during tidal breathing. These observations imply that a variation in ionic composition or possibly surface tension of the RTLF contributes to the inter-individuality. Edwards et al.[57] also suggest, based on *in vivo* and *in vitro* experiments, that delivery of surfactant to the lung, i.e., decreasing surface tension, will magnify particle expiration. On the other hand, Haslbeck et al.[48] used computational fluid dynamics to model film droplet formation, and reached the opposite conclusion; that an increased surface tension generates more droplets. The results obtained in **Paper IV** agree with Haslbeck et al.[48] as they show that high surface tension favours the formation of droplets generated from bursting fluid films. Surface tension is an important parameter when

considering rupturing fluid films, since the behaviour of a receding film after rupture is determined by the relation between surface tension and viscosity of the fluid.[65] If viscous forces are greater than surface tension driven forces, the receding film would accommodate for the liquid by increasing its thickness. No rim would be formed and the film droplet formation mechanism would be partly or completely inactivated.[69] Moreover, it appears reasonable that a greater surface tension driven force on the rim would result in an enhanced droplet formation as well as greater possibility of generating secondary droplets due to a higher impact velocity of the primary droplets as they collide with the airway wall.

Intra-individual variations in exhaled particle concentrations can be high.[1,47,56] In **Paper III**, the lowest intra-individual variations were generally found in subjects who had participated in exhaled particle studies several times previously, i.e., subjects who have had some practice. Large variations were observed in subjects who had difficulties following the prescribed breathing pattern. However, after some training reasonable to high reproducibility could be obtained.

Relation Between Humidity and Particle Size

The effect of relative humidity (RH) on particle size was studied in **Paper II**. The results show that the diameter of an exhaled particle shrinks by a factor of about 0.42 when the RH is changed from 99.5% to 75%. The results confirm the theoretical study by Nicas et al.[6], who suggested that exhaled particles shrink to approximately half their original size when leaving the human body.

Particles that are generated in the terminal bronchioles are subjected to an RH of approximately 99.5%, or better 99.48±0.01%. This value is derived from the osmolality of blood serum of 287±4 mmol kg^{-1}.[68] It was not possible, with current instrumentation, to measure particles at such high humidity. Instead, they were measured at a maximum of 71-85% RH, which is lower than what is expected in exhaled air at body temperature.[49] This observation is probably an effect of air, originating from the warm distal parts of the lungs, being temporarily cooled by the colder inner walls of the upper airways and mouth.[68,70]

Exhaled particles were measured with an OPC. The resulting number size distribution peaked in the smallest size interval of the instrument, thus a fraction of the particles was not measured. When exhaled air and particles were sent through a diffusion drier prior to measurement, lower number concentrations were reported. Water evaporated from the particles, the particles shrunk, and a larger part of the size distribution fell below the detection limit of the OPC. The changes in size or concentration did not indicate a sudden phase transition; hence the particles are expected to be supersaturated shortly after exhalation.

The addition of an oven to the set-up resulted in an apparent increase in particle concentration. This is unexpected if only size reduction caused by additional water loss is taken into account. It is possible that the apparent concentration increase reflects a transformation from a supersaturated liquid to a dry amorphous or partly crystalline solid. Assuming that exhaled particles contain a large fraction of liquid water and salts, e.g. NaCl, it is speculated that although the physical size of the particles were reduced due to further loss of water, this was more than compensated for by a more efficient light scattering in the OPC. This is so because a solid NaCl particle scatters more light than a liquid water droplet does in the size range and scattering angle studied.[71,72]

The suggestion that exhaled particles are liquid and thus supersaturated shortly after exiting the human body is supported by the images achieved by the SEM. The images show objects as large as 10-15 μm, but such large particles cannot be exhaled since they would deposit in the respiratory system on their way through it. Moreover, particles larger than 2.0 μm would impact on an earlier collection stage of the impactor. It is therefore probable that the objects seen in the images were in fact liquid, possibly viscous droplets when they impacted on the plate. After impaction, the viscous droplets spread out, wetting the impaction plate. At the centre of the plate, individual droplets may impact in the vicinity of each other, and subsequently coalesce to create larger droplets. This is less likely to occur in the periphery of the plate; consequently the objects found there are smaller, single objects. There are no traces of what may be perceived as crystalline material, and it appears that the dried droplets have a "glassy" structure.

Number Size Distribution Measurements

The study of number size distributions of exhaled particles offers a measurement challenge. Few, if any, single instruments are able to measure the whole distribution with adequate size resolution. Two or more instruments may be combined, but differences in, e.g., measurement principle, size resolution and detection efficiency then has to be taken into account. **Paper I-III** show that the size distribution of exhaled particles peaks in the lowest interval of the OPC, leaving a part of the distribution at small sizes not being measured. If an OPC is the only instrument used, it is therefore not clear what a complete distribution would look like. In **Paper I**, an SMPS was added to the set-up, and a wider size range could be measured. The SMPS measured particles between 0.01 and 0.43 μm, and the OPC from 0.41 to 33 μm, although no particles larger than 4.55 μm were detected. The distribution peaks at around 0.07 μm for tidal breathing. When breathing reaching airway closure, this mode is still present as a minor part of the distribution, but the majority of particles are found in a larger and broader mode at the upper end of the SMPS detection range. Where the SMPS and OPC measurement ranges overlap, i.e., between 0.41 and

0.43 μm, the data obtained from the SMPS have lower values than those obtained from the OPC. The overlapping part represents only a small fraction of the lower end of the smallest size interval in the OPC, while the size resolution in the data obtained by the SMPS is better. The lower SMPS values in the overlapping region indicates that the distribution peaks somewhere in the 0.41-0.55 μm interval of the OPC (the lowest interval) and has begun to fall towards the 0.41 μm detection limit.

Low concentrations also complicate measurements of exhaled particles. Individual size distributions can be obtained from the OPC in an efficient manner, as the instrument may measure all particle sizes within the detection range simultaneously. This is not possible for SMPS measurements, since this instrument only observes charged particles in a small interval of the size distribution at any given time. Thus, low concentrations necessitate long measuring times. In the present work, concentrations were too low to make statistically reliable individual size distributions within reasonable time frames. Increasing the scanning time would put undue requirements on the breathing subject and furthermore introduce the human factor as a significant uncertainty in the measurements, since it is difficult to maintain the same breathing pattern for an extended period of time. The only way to describe the size distribution below 0.41 μm in **Paper I** was therefore as an average value of all individuals under study.

RH was not monitored in **Paper I**, but it was shown in **Paper II** that exhaled particles shrink by a factor of around 0.42 when they exit the human body for a surrounding with 75% RH. Even though the experimental set-up in **Paper I** was designed to maintain the vapour concentration near that of the lung, it is likely that some shrinkage caused by a decrease in RH occurs. The modes found in **Paper I** should therefore be shifted towards larger sizes in order to represent the particles at the point of formation. Nonetheless, **Paper I** is the first publication where exhaled particles as small as 0.01 μm were measured in exhaled air. It could be argued that the low concentration of small particles reported by the SMPS was a result of leakage from the surrounding air. Even though all experimental set-ups were carefully leak-tested, there is always a risk of contamination from room air where the subject is located, or from the subject itself. Before each measurement, airways were therefore cleansed from possible residual ambient particles, by breathing clean, particle-free air for three minutes.[73] Subjects were also wearing a nose clip to prevent unfiltered room air from entering the airways. Moreover, unfiltered room air would manifest as a much broader distribution, dominating the peak found at small particle sizes. Hence, leakage cannot explain the very small particles measured in the present experiments.

Recent studies, including those presented here, agree that exhaled particles are mostly in the sub-micron size range.[1,2,47–53] It is, however, difficult to compare results presented by different authors, since both breathing method and instrumen-

tation varies. The only comprehensive study of exhaled particle size distribution available for comparison is that of Johnson and Morawska,[53] who performed experiments using breathing manoeuvres that can be expected to result in extensive airway closure. The authors measured exhaled particles with an aerodynamic particle sizer (APS) and found that size distributions peaked between 0.8 and 0.9 μm. Shrinkage of particles due to evaporation of water was considered in models, but not taken into account for actual measurements. A possible explanation to the discrepancy with current data is that the counting efficiency for the APS falls below 0.9 μm to reach 30% at the lower detection limit of 0.5 μm.[74] It is therefore possible that some of the smaller particles were lost, and that larger particles thus were overrepresented in the reported size distribution. Furthermore, differences in measurement principle and size resolution may contribute to the disagreements.

Effects of Exhalation Depth

The results presented in **Paper I** and **Paper III** show that tidal breathing, i.e., exhalation to FRC, produces lower concentrations of particles than deeper exhalations, i.e., exhalation approaching RV. This is taken as support for the suggested film rupture mechanism as a strong contributor to formation of endogenous particles in small airways. Substantially higher numbers of airways close when exhaling to RV than when exhaling to FRC, hence more liquid blockages will be able to rupture and generate particles. When exhaling to FRC, airway closure is usually not detected by conventional tests, but does take place to some extent[75] and could therefore account for the observed particles. Since expiratory flow rates were kept low, the contribution of turbulence-induced particles should be negligible.[47]

In **Paper I**, the average size distribution peaks at around 0.07 μm when exhaling to FRC. When exhaling to RV, this mode is still present, but an additional, stronger and broader mode appears between 0.2 and 0.5 μm. This indicates a change-over from one main formation mechanism to another. Moreover, the subjects who produced high concentrations of particles when exhaling to FRC did not necessarily do so when exhaling to RV. A correlation is excepted if a single mechanism is to govern the particle formation process for both breathing manoeuvres. However, the number size distributions obtained in **Paper III** show that the size distribution between 0.41 and 1.0 μm is similar regardless of breathing technique, i.e., regardless of exhaling to FRC or to RV. This would instead suggest that the formation mechanism is the same for both manoeuvres. The apparent contradictions in the two studies can be explained by the smaller detectable size in **Paper I**. If only data obtained from the OPC are considered in **Paper I**, the distribution peaks in the smallest size interval of the instrument for both breathing manoeuvres. The size distributions are similar, even though exhaling to RV results in substantially higher concentrations than exhaling to FRC. The difference in size distribution for the two breathing manoeuvres

is obvious only for particles measured with the SMPS, i.e., for particles smaller than about 0.4 μm. When exhaling to FRC, the distribution peaks at 0.07 μm and falls towards the upper detection limit of the instrument. This is not the case when exhaling to RV; the distribution instead continues to rise.

Airway closure begins in the lower regions of the lungs, where airway diameters are small, and progresses upwards as the exhalation becomes deeper.[32] It is suggested that exhaling to FRC only activates the very smallest airways. When exhaling to RV, these airways still produce particles, but the majority are generated in larger airways. A relation between airway diameter and particle size can be inferred from **Paper IV**, where fluid films spanned over small holes generated smaller droplets than those spanned over larger holes.

Effects of Breath Hold

The work performed in **Paper III** investigates the effect of breath hold on the number of exhaled particles. Breath hold at RV or FRC increases the concentration significantly, and may be explained by the consideration that airway closure is a time dependent process.[17] Assuming that particles are formed from fluid films, time is consumed when moving RTLF from the layer on the airway wall to form a liquid plug. A longer time at conditions favouring airway closure means that more liquid plugs are formed and that a larger area of film is spanned across the airways. Hence more films may rupture and form particles in the subsequent exhalation. It appears that most of the bronchioles that may close during exhalation to FRC do so within the first 5 seconds of breath hold, while 10 seconds or more are necessary to close the majority of airways when exhaling to RV.

Breath hold at TLC results in a substantial decrease in particle concentration that may be explained by deposition of particles in the airways. Particle deposition in the distal airways is a complex process. Hinds[14] suggests that alveolar sedimentation is the most important deposition process for particles larger than 0.5 μm, and that diffusion is dominating for particles smaller than 0.5 μm. Since the particles measured in **Paper III** were larger than about 0.4 μm, attempts were made to estimate the fraction of particles that would be lost through sedimentation after breath hold at TLC. Calculations show that sedimentation alone cannot account for all particle loss, but that other processes contribute as well. If the particle sizes measured by the OPC are used together with an alveolar diameter of 0.3 mm, calculations on sedimentation constantly overestimate the loss of large particles ($>$1 μm). The loss of small particles ($<$1 μm), on the other hand, is underestimated.

Sedimentation is favoured by small settling volumes and large particle sizes. It is possible that the size of the model alveolus is overestimated in the calculations,

or that the particle size is underestimated. The literature gives values of alveoli diameter ranging from 0.2 to 0.5 mm in diameter,[12,13,15] and the value used here is 0.3 mm. However, in order to account for the observed loss, the alveolar diameter used in the models has to be less than 0.05 mm, which seems very unlikely. Also, smaller alveoli would worsen the agreement between observed and predicted loss for particles larger than 1 μm. It is more likely that the sizes of the exhaled particles were underestimated in the calculations, since they probably shrank while travelling from the alveolar regions to the point of detection outside the human body. If, as an extreme case, the size reduction factor 0.42, obtained in **Paper II**, is applied to the calculations in **Paper III**, the droplets in the alveoli would have been 2.4 times larger than the measured droplet size. Thus, sedimentation would have been faster. If the increase is applied to particles smaller than about 1 μm, the calculated loss in the alveoli becomes larger and a better agreement is seen between measured and calculated loss, especially for the still air model. Shrinkage of the aqueous particles is therefore a process that would explain the observations, at least for particles smaller than 1 μm. An increase in diameter due to higher RH would again worsen the agreement for larger particles.

In summary, gravitational settling in the alveoli and shrinkage of particles upon a change in RH may explain the loss of particles smaller than 1 μm, but not the loss of particles larger than that. It is likely that several concurrent processes should be taken into account. Sedimentation and diffusion are both mechanisms that are favoured by small alveoli sizes, giving short transport distances to a wall were deposition may take place. In the calculations performed here, the alveoli are assumed to be spherical. Elongated structures with the main axis in the vertical wall direction may allow a contribution to loss of small particles from diffusion in the horizontal direction while reducing the loss of larger particles since the distance to the nearest surface in the vertical direction is increased.

Influence of Film Dimensions

Airway closure and subsequent reopening is generally considered to take place in the terminal bronchioles, i.e., at diameters of around 0.6 mm,[28,29] and Macklem et al.[76] were able to observe liquid menisci in airways smaller than 0.5 mm in excised cat lung lobes. However, it has not been obvious that the film droplet formation mechanism will work at such small diameters.

Theoretically, the number of droplets generated from a fluid film should approach zero as the film diameter decreases, simply because there is less and less material available for generating the droplets. This is confirmed by the results in **Paper IV**, but is not the case for SDFC. It appears that the ability to generate droplets does not depend on film diameter, at least not for diameters down to 0.95 mm. Thus, film

droplet formation may take place for fluid films smaller than that. This information can be applied to make statements about where in the airways exhaled particles may or may not be generated.

The fact that the smallest droplets were generated from the smallest film diameters suggests that the smallest airways generate the smallest exhaled particles. This is supported by the results from **Paper I**, where exhaling to FRC resulted in the generation of smaller particles than exhalation to RV. Since airway closure begins in the lower regions of the lungs,[32] where airway diameters are small, it is possible that very small airways close when exhaling to FRC. As exhalation approaches RV, larger airways close and larger particles are generated. Particles from the smallest airways still contribute to the total amount, but the contribution from larger airways dominates.

When a flat fluid film ruptures, droplets are formed from the receding edge of the film. The edge moves towards the inside walls of the holes in the plates described in **Paper IV**. If the ratio between plate thickness and hole diameter is large, it is expected that many droplets impact on the wall and are lost or possibly generate secondary droplets. In **Paper IV**, the thick plates generally gave fewer droplets than the thin ones. This may thus be explained by impaction and loss of droplets. As a comparison, the typical physiological length to diameter ratio in small airways is about 2-3,[77] much larger than the ratio ($\ll 1$) tested here. Hence, it is possible that an even larger fraction of film droplets will impact on the airway wall and never be exhaled. Small secondary droplets may, however, also be of interest when considering small particles originating from the airways.

Concluding Remarks and Outlook

The work performed in this thesis was undertaken with the intention to extend the knowledge about the formation mechanisms and physical behaviour of exhaled aerosol particles. The results from the different studies support the hypothesis that film droplet formation is a strong contributor to endogenous particle production. Film droplet formation is expected to take place following airway closure, which normally occurs in the region of the terminal bronchioles. Consequently, exhaled particles originate from this region, and thus carry information about the composition of RTLF in the distal airways. It is also suggested that exhaled particles leave the body as concentrated, supersaturated, possibly viscous droplets, and that they quickly equilibrate to the surrounding environment.

Number size distributions of exhaled particles depend on the type of breathing employed. Exhaling to FRC (tidal breathing) results in fewer and smaller particles than exhaling to RV (breathing reaching airway closure). Thus, it is possible that the manoeuvres generate particles originating from different regions of the small airways. It is proposed that tidal breathing activates only the smallest airways, while exhaling reaching airway closure includes additional airways, progressing in size. If exhaled aerosol sampling is to be used as a diagnostic tool in, e.g., medicine, it is therefore necessary to standardise the measurement method and the breathing manoeuvre employed. Sampling should be performed while monitoring inhalation and exhalation flow rates in real time. It is also desirable to characterise the breathing subject prior to particle collection, to find, e.g., closing point. This way, the process of exhaled particle collection can be carefully controlled. For ensuing chemical analysis, as high concentrations of particles as possible are needed. For this purpose, it is suggested that the subject under investigation exhales to RV rather than to FRC. In order to maximise the number of particles emitted, exhalation should be ended by a short period of breath hold, subsequent inhalation to TLC, immediately followed by slow exhalation.

Information about physical properties of exhaled particles is still lacking. For full characterisation, an instrument that can measure the whole distribution at once,

with acceptable size resolution, is desired. No such instrument exists at present. Moreover, since exhaled particles quickly evaporate when they leave the human body, relative humidity should be monitored so that shrinkage due to evaporation of water can be corrected for. Again, well defined breathing manoeuvres are essential to produce data with high statistical credibility.

If the requirements described above are taken into consideration, exhaled particles have the potential for becoming important tools when diagnosing, monitoring and screening various medical conditions.

Acknowledgements

Här kommer delen där man får bli lite mer personlig. Då gäller det att passa på.

Jag vill tacka min handledare **Evert** som har stor del i att denna avhandling blivit skriven. När jag står handfallen kommer du med silvertejp, ståltråd, entusiastiska förslag och glada tillrop; det uppskattas. På tal om entusiasm så tackar jag för samarbetet med **arbets- och miljömedicin**, där tankar och idéer är nästan oändligt många. Särskilt tack till **Anna-Carin**, **Lotta** och **Per** som bidragit till såväl diskussioner som publikationer, och även till den tvärvetenskaplighet jag känner att jag börjar uppnå. Detsamma gäller **Björn** på Sahlgrenska, den stora kunskapskällan då det gäller luftvägar. Vidare så hade det varit omöjligt att utföra mina experiment om det inte vore för alla förstående och tålmodiga **försökspersoner**.* Tack för att ni stod ut!

Jag kommer att sakna mina arbetskamrater på **atmosfärsvetenskap**, som jag har haft mycket roligt med under såväl arbetstid som fritid. Jag skickar också en hälsning till mina "riktiga" kollegor på **oorganisk miljökemi** och tackar för att jag fick komma på era fester trots att jag prioriterade bort nästan alla möten. Tack till **Göteborgs miljövetenskapliga centrum (GMV)** som finansierat dessa studier.†

Det har varit lite mycket laborerande, artikelskrivande och avhandlingsarbete på senare tid, och jag vill därför tacka mina **vänner** för att ni fortfarande vill vara mina vänner.‡ Nu ska vi fika och umgås så att det står härliga till. **Familjen**, biologisk som utökad, har bidragit till att det här blev av. Lite extra sentimentalt och kletigt tack till bäste **Frans** för vallning och obegränsat stöd då jag behövt det som mest.§

∴ Tack till alla **medarbetare** och **medmänniskor**.

*det känns som om jag skulle bryta mot någon slags etisk forskningssekretess om jag nämner era namn... men... ni vet vilka ni är; tack.

†Adlerbertska forskningsstiftelsen har också bidragit.

‡extra tack till Linda, Anna, Ågren och Frans för att ni med kritiskt öga ifrågasatt meningsbyggnader, grammatik och prepositioner i denna avhandling; jag håller er ansvariga för erratan!

§även motvilligt, tveksamt tack för skarpa tillsägningar då det varit det enda alternativet.

Bibliography

1. Almstrand A-C, Ljungström E, Lausmaa J, Bake B, Sjövall P, and Olin A-C: Airway monitoring by collection and mass spectrometric analysis of exhaled particles. Anal Chem. 2009;81:662-668.
2. Papineni RS and Rosenthal FS: The size distribution of droplets in the exhaled breath of healthy human subjects. J Aerosol Med. 1996;10:105-116.
3. Hunt J: Exhaled breath condensate: An evolving tool for noninvasine evaluation of lung disease. J Allergy Clin Immunol. 2002;110:28-34.
4. Scheideler L, Manke HG, Schwulera U, Inacker O, and Hammerle H: Detection of nonvolatile macromolecules in breath - a possible diagnostic tool? Am Rev Respir Dis. 1993;148:778-784.
5. Riley RL: Airborne infection. Am J Med. 1974;57:466-475.
6. Nicas M, Nazaroff WW, and Hubbard A: Toward understanding the risk of secondary airborne infection: Emission of respirable pathogens. J Occup Environ Hyg. 2005;2:143-154.
7. Mutlu GM, Garey KW, Robbins RA, Danziger LH, and Rubinstein I: Collection and analysis of exhaled breath condensate in humans. Am J Respir Crit Care Med. 2001;164:731-737.
8. Horvath I, Hunt J, and Barnes PJ: Exhaled breath condensate: Methodological recommendations and unresolved questions. Eur Respir J. 2005;26:523-548.
9. Effros RM, Hoagland KW, Bosbous M, Castillo D, Foss B, Dunning M, Gare M, Lin W, and Sun F: Dilution of respiratory solutes in exhaled condensates. Am J Respir Crit Care Med. 2002;165:663-669.
10. Levitzky MG: Function & structure of the respiratory system. In: Pulmonary physiology, McGraw-Hill Medical Publishing Division: Blacklick, OH, USA. pp. 1-21, 2007.
11. Whipp BJ: Pulmonary ventilation. In: Comprehensive human physiology - from cellular mechanisms to integration, edited by Greger R and Windhurst U, Springer: Berlin-Heidelberg, Germany, pp. 2015-2036, 1996.
12. Wang N-S: Anatomy and ultrastructure of the lung. In: Pulmonary biology in health and disease, edited by Bittar EE, Springer: Secaucus, NJ, USA. pp. 13-31, 2002.
13. Ochs M, Nyengaard LR, Lung A, Knudsen L, Voigt M, Wahlers T, Richter J, and Gundersen HJG: The number of alveoli in the human lung. Am J Respir Crit Care Med. 2004;169:120-124.
14. Hinds WC: Aerosol technology - properties, behaviour, and measurements of airborne particles. John Wiley & Sons Inc.: New York, USA, 1982.
15. Weibel ER: Morphometry of the human lung. Springer: Berlin-Göttningen-Heidelberg, Germany, 1963.
16. Phillips CG and Kaye SR: On the asymmetry of bifurcations in the bronchial tree. Respir Physiol. 1997;107:85-98.
17. Heil M, Hazel AL, and Smith JA: The mechanics of airway closure. Respir Physiol Neuro. 2008;163:214-221.

18. Connor LM, Bidani A, Goerke J, Clements JA, and Postlethwait EM: NO_2 interfacial transfer is reduced by phospholipid monolayers. J Appl Physiol. 2001;91:2024-2034.
19. Ng AW, Bidani A, and Herring TA: Innate host defense of the lung: Effects of lung-lining fluid pH. Lung. 2004;182:297-317.
20. Lucas A and Douglas L: Principles underlying ciliary activity in the respiratory tract. II. A comparison of nasal clearance in man, monkey and other mammals. Arch Otolaryngol Head Neck Surg. 1934;20:518-541.
21. Kim WD: Lung mucus: A clinician's view. Eur Respir J. 1997;10:1914-1917.
22. Wright SM, Hockey PM, Enhorning G, Strong P, Reid KBM, Holgate ST, Djukanovic R, and Postle AD: Altered airway surfactant phospholipid composition and reduced lung function in asthma. J Appl Physiol. 2000;89:1283-1292.
23. Poynter SE and LeVine AM: Surfactant biology and clinical application. Crit Care Clin. 2003;19:459-472
24. Gilljam H, Andersson O, Ellin A, Robertson B, and Strandvik B: Composition and surface-properties of the bronchial lipids in adult patients with cystic-fibrosis. Clin Chim Acta. 1988;176:29-37.
25. Yager D: Airway wall liquid in health and disease. In: Pulmonary biology in health and disease, edited by Bittar EE, Springer-Verlag: New York, USA. pp. 250-264, 2002.
26. Levitzky MG: Mechanics of breathing. In: Pulmonary physiology, McGraw-Hill Medical Publishing Division: Blacklick, OH, USA. pp. 22-61, 2007.
27. Seinfeld JH and Pandis SN: Atmospheric chemistry and physics - from air pollution to climate change. John Wiley & Sons Inc.: New York, USA, 1998.
28. Hughes JMB, Rosenzwe DY, and Kivitz PB: Site of airway closure in excised dog lungs: Histologic demonstration. J Appl Physiol. 1970;29:340-339.
29. Macklem PT: Airway obstruction and collateral ventilation. Physiol Rev. 1971;51:368-436.
30. Alencar AM, Majumdar A, Hantos Z, Buldyrev SV, Stanley HE, and Suki B: Crackles and instabilities during lung inflation. Physica A. 2005;357:18-26.
31. Pasterkamp H, Kraman SS, and Wodicka GR: Respiratory sounds - advances beyond the stethoscope. Am J Respir Crit Care Med. 1997;156:974-987.
32. Dollfuss RE, Milic-Emili J, and Bates DV: Regional ventilation of lung studied with boluses of 133xenon. Respir Physiol. 1967;2:234-246.
33. Milic-Emili J, Torchio R, and D'Angelo E: Closing volume: A reappraisal (1967-2007). Eur J Appl Phys. 2007;99:567-583.
34. Turner JM, Mead J, and Wohl ME: Elasticity of human lungs in relation to age. J Appl Physiol. 1968;25:664-671.
35. Kamm RD and Schroter RC: Is airway-closure caused by a liquid-film instability? Respir Physiol. 1989;75:141-156.
36. Halpern D, Fujioka H, and Grotberg JB: The effect of viscoelasticity on the stability of a pulmonary airway liquid layer. Phys Fluids. 2010;22.
37. Halpern D and Grotberg JB: Surfactant effects on fluid-elastic instabilities of liquid-lined flexible tubes - a model of airway-closure. Journal of Biomechanical Engineering-Transactions of the ASME. 1993;115:271-277.
38. Otis DR, Petak F, Hantos Z, Fredberg JJ, and Kamm RD: Airway closure and reopening assessed by the alveolar capsule oscillation technique. J Appl Physiol. 1996;80:2077-2084.
39. Cassidy KJ, Halpern D, Ressler BG, and Grotberg JB: Surfactant effects in model airway closure experiments. J Appl Physiol. 1999;87:415-427.
40. Malashenko A, Tsuda A, and Haber S: Propagation and breakup of liquid menisci and aerosol generation in small airways. J Aerosol Med Pulm Drug Deliv. 2009;22:341-353.
41. Lindsley WG, Collicott SH, Franz GN, Stolarik B, McKinney W, and Frazer DG: Asymmetric and axisymmetric constant curvature liquid-gas interfaces in pulmonary airways. Ann Biomed Eng. 2005;33:365-375.

42. Phillips M, Altorki N, Austin JHM, Cameron RB, Cataneo RN, Greenberg J, Kloss R, Maxfield RA, Pass HI, Rom WN, and Tietje O: Prediction of lung cancer using volatile biomarkers in breath. J Clin Oncol. 2005;23:839S-839S.
43. Phillips M, Cataneo RN, Ditkoff BA, Fisher P, Greenberg J, Gunawardena R, Kwon CS, Tietje O, and Wong C: Prediction of breast cancer using volatile biomarkers in the breath. Breast Cancer Res Treat. 2006;99:19-21.
44. Bondesson E, Jansson LT, Bengtsson T, and Wollmer P: Exhaled breath condensate - site and mechanisms of formation. J Breath Res. 2009;3:1-5.
45. Jennison MW: In: Aerobiology, edited by Moulton FR, Amer Assoc Adv Sci Pub: Washington, DC, USA, 1942.
46. Duguid JP: The size and the duration of air-carriage of respiratory droplets and droplet-nuclei. J Hyg. 1946;44:471-479.
47. Almstrand A-C, Bake B, Ljungström E, Larsson P, Bredberg A, Mirgorodskaya E, and Olin A-C: Effect of airway opening on production of exhaled particles. J Appl Physiol. 2010;108:584-588.
48. Haslbeck K, Schwarz K, Hohlfeld JM, Seume JR, and Koch W: Submicron droplet formation in the human lung. J Aerosol Sci. 2010;41:429-438.
49. Morawska L, Johnson GR, Ristovski ZD, Hargreaves M, Mengersen K, Corbett S, Chao CYH, Li Y, and Katoshevski D: Size distribution and sites of origin of droplets expelled from the human respiratory tract during expiratory activities. J Aerosol Sci. 2009;40:256-269.
50. Schwarz K, Biller H, Windt H, Koch W, and Hohlfeld JM: Characterization of exhaled particles from the healthy human lung - a systematic analysis in relation to pulmonary function variables. J Aerosol Med Pulm Drug Deliv. 2010;23:371-379.
51. Fairchild CI and Stampfer JF: Particle concentration in exhaled breath - summary report. Am Ind Hyg Assoc J. 1987;48:948-949.
52. Gebhart J, Anselm A, Heyder J, and Stahlhofen W: The human lung as aerosol particle generator. J Aerosol Med. 1988;1:196-197.
53. Johnson GR and Morawska L: The mechanism of breath aerosol formation. J Aerosol Med Pulm Drug Deliv. 2009;22:1-9.
54. Yang SH, Lee GWM, Chen CM, Wu CC, and Yu KP: The size and concentration of droplets generated by coughing in human subjects. J Aerosol Med. 2007;20:484-494.
55. Chao CYH, Wan MP, Morawska L, Johnson GR, Ristovski ZD, Hargreaves M, Mengersen K, Corbett S, Li Y, Xie X, and Katoshevski D: Characterization of expiration air jets and droplet size distributions immediately at the mouth opening. J Aerosol Sci. 2009;40:122-133.
56. Johnson GR, Morawska L, Ristovski ZD, Hargreaves M, Mengersen K, Chao CYH, Wan MP, Li Y, Xie X, Katoshevski D, and Corbett S: Modality of human expired aerosol size distributions. J Aerosol Sci. 2011;42:839-851.
57. Edwards DA, Man JC, Brand P, Katstra JP, Sommerer K, Stone HA, Nardell E, and Scheuch G: Inhaling to mitigate exhaled bioaerosols. Proc Natl Acad Sci U S A. 2004;101:17383-17388.
58. Moriarty JA and Grotberg JB: Flow-induced instabilities of a mucus-serous bilayer. J Fluid Mech. 1999;397:1-22.
59. Kleinstreuer C, Zhang Z, and Kim CS: Combined inertial and gravitational deposition of microparticles in small model airways of a human respiratory system. J Aerosol Sci. 2007;38:1047-1061.
60. Blanchard DC: The electrification of the atmosphere by particles from bubbles in the sea. Progr Oceanogr. 1963;1:73-202.
61. Spiel DE: On the births of film drops from bubbles bursting on seawater surfaces. J Geophys Res - Oceans. 1998;103:24907-24918.
62. Roisman IV, Horvat K, and Tropea C: Spray impact: Rim transverse instability initiating fingering and splash, and description of a secondary spray. Phys Fluids. 2006;18:19.

63. Mårtensson EM, Nilsson ED, de Leeuw G, Cohen LH, and Hansson H-C: Laboratory simulations and parameterization of the primary marine aerosol production. J Geophys Res - Atmos. 2003;108:12.
64. O'Dowd CD and de Leeuw G: Marine aerosol production: A review of the current knowledge. Phil Trans R Soc A. 2007;365:1753-1774.
65. McEntee WR and Mysels KJ: Bursting of soap films. I. An experimental study. J Phys Chem. 1969;73:3018-3028.
66. Lhuissier H and Villermaux E: Soap films burst like flapping flags. Phys Rev Lett. 2009;103:4.
67. TSI Incorporated, Instruction manual model 3071 electrostatic classifier. 1977: MN, USA.
68. Ferron GA, Haider B, and Kreyling WG: Inhalation of salt aerosol particles - I. Estimation of the temperature and relative humidity of the air in the human upper airways. J Aerosol Sci. 1988;19:343-363.
69. Watanabe W, Thomas M, Clarke R, Klibanov AM, Langer R, Katstra J, Fuller GG, Griel LC, Fiegel J, and Edwards D: Why inhaling salt water changes what we exhale. J Colloid Interface Sci. 2007;307:71-78.
70. Hanna L and Scherer P: Regional control of local airway heat and vapor losses. J Appl Physiol. 1986;61:624-632.
71. Schneider F, Charakterisierung von aerosolpartikeln aus der landwirtschaft, in Forschungsbericht Agrartechnik des Arbeitskreises Forschung und Lehre der Max-Eyth-Gesellschaft Agrartechnik im VDI (VDI-MEG). 2005, Universität Hohenheim: Selbstverlag.
72. Perry RJ, Hunt AJ, and Huffman DR: Experimental determinations of mueller scattering matrices for nonspherical particles. Applied Optics. 1978;17:2700-2710.
73. Invernizzi G, Ruprecht A, De Marco C, Paredi P, and Boffi R: Residual tobacco smoke: Measurement of its washout time in the lung and of its contribution to environmental tobacco smoke. Tob Control. 2007;16:29-33.
74. Armendariz AJ and Leith D: Concentration measurement and counting efficiency for the aerodynamic particle sizer 3320. J Aerosol Sci. 2002;33:133-148.
75. Forkert L, Dhingra S, and Anthonisen NR: Airway-closure and closing volume. J Appl Physiol. 1979;46:24-30.
76. Macklem PT, Proctor DF, and Hogg JC: The stability of peripheral airways. Respir Physiol. 1970;8:191-203.
77. Lee JW, Kang MY, Yang HJ, and Lee E: Fluid-dynamic optimality in the generation-averaged length-to-diameter ratio of the human bronchial tree. Med Biol Eng Comput. 2007;45:1071-1078.